Bioorganic & Medicinal Chemistry xxx (xxxx) xxx–xxx

Contents lists available at ScienceDirect

Bioorganic & Medicinal Chemistry

journal homepage: www.elsevier.com/locate/bmc

Synthesis of 4′-*C*-aminoalkyl-2′-*O*-methyl modified RNA and their biological properties

Kana Koizumi[a,f], Yusuke Maeda[a,f], Toshifumi Kano[a], Hisae Yoshida[e], Taiichi Sakamoto[d], Kenji Yamagishi[e], Yoshihito Ueno[a,b,c,*]

[a] *Course of Applied Life Science, Faculty of Applied Biological Sciences, Gifu University, Japan*
[b] *United Graduate School of Agricultural Science, Gifu University, Japan*
[c] *Center for Highly Advanced Integration of Nano and Life Sciences (G-CHAIN), Gifu University 1-1 Yanagido, Gifu 501-1193, Japan*
[d] *Faculty of Advanced Engineering, Chiba Institute of Technology, 2-17-1 Tsudanuma, Narashino, Chiba 275-0016, Japan*
[e] *Department of Chemical Biology and Applied Chemistry, College of Engineering, Nihon University, 1 Aza-nakagawara, Tokusada, Tamuramachi, Koriyama, Fukushima 963-8642, Japan*

ARTICLE INFO

Keywords:
Oligonucleotide
RNA
RNA interference
Small interfering RNA
Aminoalkyl groups
Thermal stability
Nuclease resistance

ABSTRACT

In this paper, we describe the synthesis of 4′-*C*-aminoalkyl-2′-*O*-methylnucleosides and the properties of RNAs containing these analogs. Phosphoramidites of 4′-*C*-aminoethyl and 4′-*C*-aminopropyl-2′-*O*-methyluridines were prepared using glucose as starting material, and RNAs containing the analogs were synthesized using the phosphoramidites. Thermal denaturation studies revealed that these nucleoside analogs decreased the thermal stabilities of double-stranded RNAs (dsRNAs). Results of NMR, molecular modeling, and CD spectra measurements suggested that 4′-*C*-aminoalkyl-2′-*O*-methyluridine adopts an C2′-*endo* sugar puckering in dsRNA. The 4′-*C*-aminoalkyl modifications in the passenger strand and the guide strand outside the seed region were well tolerated for RNAi activity of siRNAs. Single-stranded RNAs (ssRNAs) and siRNAs containing the 4′-*C*-aminoethyl and 4′-*C*-aminopropyl analogs showed high stability in buffer containing bovine serum. Thus, siRNAs containing the 4′-*C*-aminoethyl and 4′-*C*-aminopropyl analogs are good candidates for the development of therapeutic siRNA molecules.

1. Introduction

The discovery of RNA interference (RNAi) by Fire et al. has focused research on the potential use of small interfering RNA (siRNA) as therapeutic agents.[1–3] siRNAs comprise 19–21 base pairs of double stranded RNA (dsRNA) with two 3′ nucleotide overhangs. The guide strand of the siRNA binds with Argonaute 2 protein (Ago2) to form the RNA-induced silencing complex (RISC), which in turn causes endonucleolytic cleavage of the complementary target mRNA.[4–7] siRNAs can be rationally designed and synthesized if the sequences of the target disease-causing genes are known, so that siRNAs have been regarded as novel potential therapeutic agents. Several siRNA drugs are currently being evaluated in clinical trials for the treatment of diseases, such as age-related macular degeneration (AMD),[8,9] diabetic macular edema (DME),[10] glaucoma, hypercholesterolemia, and human solid tumor (melanoma).[11]

However, clinical applications of siRNAs have been limited by several challenges. In general, siRNAs are easily degraded by nucleases present in the blood, tissues, and cells.[12] Moreover, the hydrophilic nature and negative charges of siRNAs prevent them from easily crossing the cell membrane.[13] As a result, various chemical modifications for siRNAs have been attempted to overcome these problems.[14] For example, siRNAs are commonly subjected to 2′-*O*-methyl[15,16] and 2′-fluoro[17,18] modifications, which increase the stability of siRNAs in serum. These modifications are also known to inhibit immune stimulation of siRNAs and increase the thermal stability of double-stranded RNAs (dsRNAs).[15] Furthermore, so far, synthesis of many types of 2′-*O*-aminoalkyl modified nucleic acids were reported.[19–21] The positively charged amino groups of the aminoalkyl linkers can neutralize the negative charges of oligonucleotides (ONs) and interact with the negatively charged cell membrane, causing enhancement of the cell membrane permeability of ONs.[19] However, Ago2 strictly recognizes the backbone of siRNA, especially the phosphates and hydroxy groups of the sugar moieties.[22,23] Therefore, incorporation of large functional groups at the 2′-hydroxy group of siRNA will interfere with RISC formation.

* Corresponding author.
E-mail address: uenoy@gifu-u.ac.jp (Y. Ueno).
[f] These authors contributed equally to this work.

https://doi.org/10.1016/j.bmc.2018.05.025
Received 14 April 2018; Received in revised form 17 May 2018; Accepted 17 May 2018

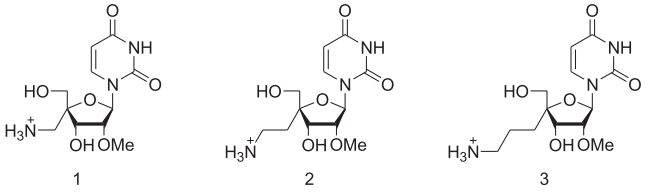

Fig. 1. Structures of the nucleoside analogs.

Matsuda and his co-workers reported the synthesis of 4′-*C*-aminoalkyl-modified DNAs.[24,25] Incorporation of aminoalkyl groups, especially the aminoethyl and aminopropyl groups, at the 4′-positions of sugar moieties was found to markedly increase the resistance of DNAs to nucleolytic degradation by both endonucleases and exonucleases.[24,26] Recently, Pradeepkumar et al. reported the synthesis of 4′-*C*-aminomethyl-2′-*O*-methyluridine (**1**) and 4′-*C*-aminomethyl-2′-*O*-methylcytidine (Fig. 1).[27] The siRNAs containing these analogs were less thermally stable but more nuclease-resistant than unmodified siRNAs. Furthermore, siRNAs harboring modifications at the passenger strands or the 3′-end of the guide strands still retained RNAi activity.

It was reported that the DNAs with longer aminoalkyl groups, such as the aminoethyl and aminopropyl groups, at the 4′-positions of sugar moieties were more nuclease-resistant than DNAs with shorter aminoalkyl groups, such as the aminomethyl group.[26] Thus, siRNAs incorporated with longer aminoalkyl groups at the 4′-position were expected to exhibit greater resistance to nucleolytic degradation by nucleases.

In the present study, we designed and synthesized RNAs and siRNAs containing 4′-*C*-aminoethyl-2′-*O*-methyluridine (**2**) and 4′-*C*-aminopropyl-2′-*O*-methyluridine (**3**) (Fig. 1). We then investigated the effects of 4′-*C*-aminoalkyl modifications on thermal stability, stability in serum, and RNAi activity of RNAs or siRNAs.

2. Results and discussion

2.1. Synthesis of nucleoside analogs

4′-*C*-aminoethyl-2′-*O*-methyl-modified uridine (**2**) and 4′-*C*-aminopropyl-2′-*O*-methyl-modified uridine (**3**) were synthesized from ribofuranose derivatives **4** and **7b** as starting material following a previously reported method[28] (Schemes 1 and 2). The ribofuranose derivative **4** prepared from D-glucose was converted to the hydroxyethyl derivative **6** via Wittig reaction and hydroboration, followed by oxidation with 63% yield (after 2 steps). Tosylation of the hydroxy group of **6** produced **7a** at 81% yield. We attempted to convert compound **7a** to the azide derivative **9a** via azidation, followed by acetolysis. However, this process generated many byproducts, which was attributed to the reaction between the tosyl group and the 3′-benzyloxy group of **7a**. To solve this problem, acetolysis was carried out before azidation. Acetolysis and azidation of **7a** produced **9a** at 74% yield (after two steps). Compound **9a** was then subjected to modified Vorbrüggen reaction[29] using *in situ* silylation of uridine and subsequent trimethylsilyl triflate-mediated coupling to produce **10a** at 85% yield. The acetate group of **10a** was hydrolyzed using concentrated (conc.) NH_3 solution in methanol to produce **11a** at 98% yield. Then, the 2′-hydroxy group of **11a** was methylated via treatment with MeI and NaH in THF at 0 °C to produce **12a** at 67% yield. Debenzylation of **12a** was carried out using BCl_3 in CH_2Cl_2 at −78 °C to produce **13a** at 78% yield. The silyl group of **13a** was removed via treatment with tetra-*n*-butylammonium fluoride (TBAF) in THF to produce **14a** at 97% yield. The 5′-OH group of **14a** was protected by a 4,4′-dimethoxytrityl (DMTr) group to produce **15a** at 96% yield.[30] The azide group of **15a** was reduced via treatment with PPh_3 in THF at 45 °C, and the resulting amino group was protected with a trifluoroacetyl (TFA) group to produce **17a** at 96% yield (after two steps).[31] Compound **17a** was phosphitylated following a standard procedure to produce the corresponding phosphoramidites **18a** at 69% yield.[32] In a similar manner, ribofuranose derivative **7b** was converted to **18b**. The total yields of **18a** and **18b** were 2.9% (after 22 steps) and 4.1% (after 22 steps), respectively. The phosphoramidite of the aminomethyl analog **1** was synthesized following a previously reported method.[27] To incorporate **17a** and **17b** into the 3′-end of the RNA oligomer, **17a** and **17b** were further modified to produce the corresponding 3′-succinates **20a** and **20b**, which were then reacted with controlled pore glass (CPG) to produce the solid supports **21a** and **21b** containing **20a** (44 μmol/g) and **20b** (36 μmol/g), respectively (Scheme 3).

2.2. Synthesis of RNA oligomers

RNA oligomers containing nucleoside analogs **1**, **2**, and **3** were successfully synthesized via standard solid phase RNA synthesis using a DNA/RNA synthesizer. Cleavage and deprotection of the oligomers were carried out via treatment of CPG beads with 10% dimethylamine in MeCN, followed by conc. NH_3 solution/40% methylamine (1:1, v/v) to prevent the additional reaction of acrylonitrile with 4′-*C*-aminoalkyl groups. After desilylation, oligomers were purified via 20% denaturing polyacrylamide gel electrophoresis (PAGE). The oligonucleotide (ON) sequences used in this study are depicted in Tables 1–3 and S1–S7.

2.3. Thermal denaturation study

First, we evaluated the effect of 4′-*C*-aminoalkyl-2′-*O*-methyl modifications on the thermal stability of dsRNAs (dsRNA **1**–**4**). UV melting experiments were performed in buffer containing 10 mM sodium phosphate (pH 7.0) and 100 mM NaCl (Fig. S1). The melting temperature (T_m) values are shown in Table 1. The T_m of natural 11-mer dsRNA **1** was 43.5 °C, whereas that of dsRNA **2**, dsRNA **3**, and dsRNA **4** containing 4′-*C*-aminoalkyl-2′-*O*-methyl modifications were 37.6, 37.3, and 36.6 °C, respectively. Incorporation of these modifications decreased the T_m values of dsRNAs by 2.0–2.3 °C/modification. Then, incorporation of 4′-*C*-aminoethyl-2′-*O*-methyl and 4′-*C*-aminopropyl-2′-*O*-methyluridine was found to decrease the thermal stability of dsRNAs, similar to the effect observed for 4′-*C*-aminomethyl-2′-*O*-methyluridine/cytosine. These modifications might influence the conformation of the sugar and hydration in the minor groove and disturb duplex formation.[25] Longer side chain lengths were found to produce lower T_m values.

Modified siRNAs were also observed to exhibit reduced thermal stability (Fig. S2 and Table 2). The T_m value of natural siRNA (siRNA **1**) was 79.5 °C, whereas those of siRNA **2**, siRNA **3** and siRNA **4** were 65.7, 65.0 and 64.6 °C, respectively. The ΔT_m values of these siRNAs were approximately −1.1 to −1.2 °C/modification, which were different from those observed for dsRNAs and were found to be dependent on the dsRNA sequence. Modification of dsRNAs with homopurine/homopyrimidine sequence was found to decrease their thermal stabilities. Destabilization of the DNA/RNA duplexes containing the 4′-*C*-aminoalkyl modification, which are composed of a mixed sequence, was lower than those containing a homopurine/homopyrimidine sequence.[23] These results suggested that the siRNAs with 4′-*C*-aminoalkyl modifications can form stable duplexes under biological conditions.

Furthermore, we carefully examined the stability of the duplexes by calculating the thermodynamic parameters of duplex formation based on the slope of the plot of $1/T_m$ vs. ln (C_T/4), where C_T is the total concentration of single-stranded RNAs (Fig. S3 and Table 3). The $\Delta G^\circ_{37^\circ C}$ value of dsRNA **5** was −10.6 kcal/mol, while those of dsRNA **9**, dsRNA **13** and dsRNA **17** were −10.1, −10.0, and −9.8 kcal/mol, respectively. The ΔS° value of dsRNA **5** was −245.7 kcal/mol·K, whereas those of dsRNA **9**, dsRNA **13** and dsRNA **17** were −261.8, −266.1, and −272.2 kcal/mol·K, respectively. These results indicated that the thermodynamic destabilization of the duplexes was caused by disadvantages in terms of entropy (ΔS°). In addition, longer side chain

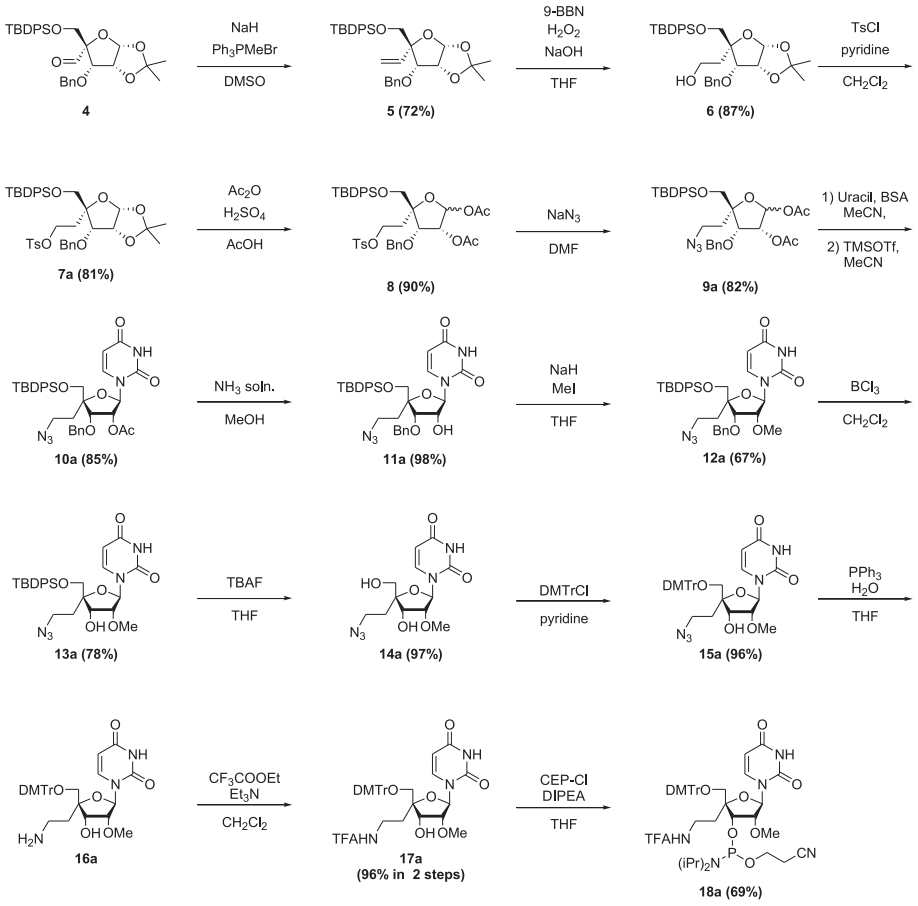

Scheme 1. Synthesis 4′-*C*-aminoethyl-2′-*O*-methyluridine phosphoramidite **18a**.

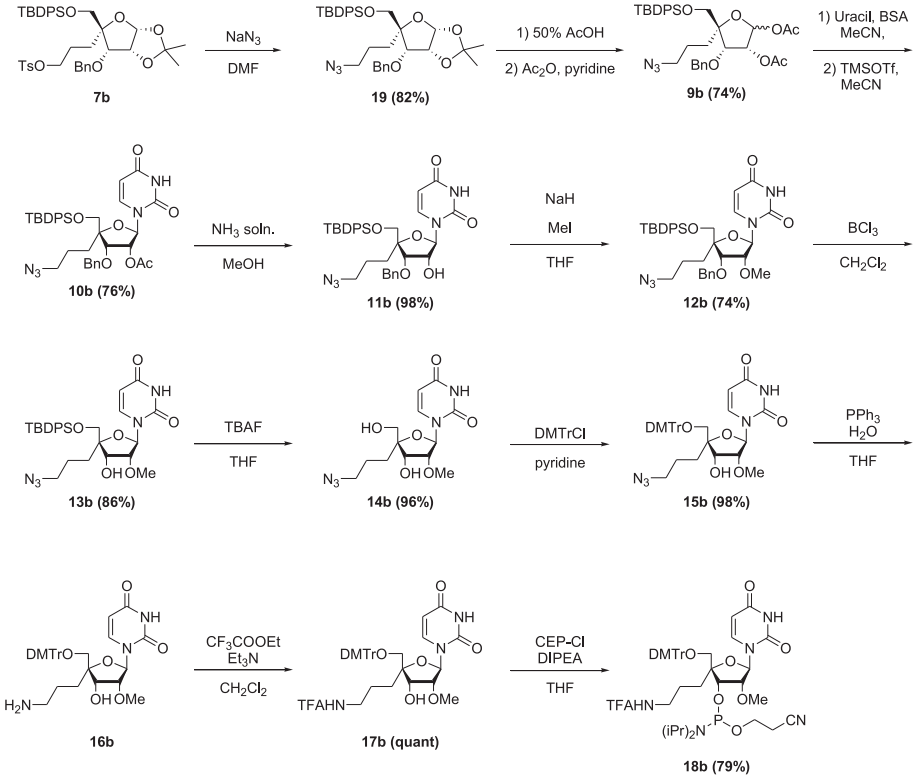

Scheme 2. Synthesis of 4′-*C*-aminopropyl-2′-*O*-methyluridine phosphoramidite **18b**.

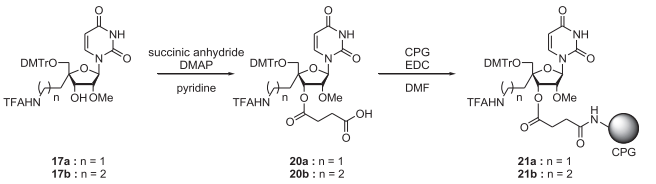

Scheme 3. Synthesis of the controlled-pore glasses (CPGs) **21a** and **21b** carrying **17a** and **17b**.

lengths resulted in more unfavorable entropy, which suggested that 4′-*C*-aminoalkyl modification induces conformational changes that interfere with the duplex formation.

Next, we assessed the base-discriminating abilities of dsRNAs (Table S1 and Fig. 2). The ΔT_m (T_m of duplex containing mismatched base pair $-T_m$ of complementary duplex) values for the natural duplexes (dsRNA **6–8**) were −5.4 to −11.8 °C, whereas those for the duplexes harboring the modifications (dsRNA **10–12**, dsRNA **14–16** and dsRNA **18–20**) were −7.6 to −12.1 °C. Thus, the 4′-*C*-aminoalkyl-2′-*O*-methyluridines had base-discriminating abilities in dsRNA.

2.4. NMR measurements

We performed NMR measurements to evaluate the sugar puckering of 4′-*C*-aminoethyl-2′-*O*-methyluridine (**2**). First, the monomer population in the C2′-*endo* conformation was calculated from $J_{1'\text{-}2'}$. The calculated percentages of 4′-*C*-azidoethyl-2′-*O*-methyluridine (**14a**) and 4′-*C*-azidopropyl-2′-*O*-methyluridine (**14b**) in the C2′-*endo* conformation were 69.0% and 68.4%, respectively.

Next, the sugar puckering of 4′-*C*-amiNOEthyl-2′-*O*-methyluridine (**2**) in dsRNA was directly measured via NMR. The NMR signals of non-exchangeable base protons (H2/H5/H6/H8) and ribose H1′ of 5′-CGC GAAU**2**CGCG-3′ were assigned via the well-established sequential NOE connectivity method (Fig. S4).[33] NMR assignments were compared to previously reported NMR data.[34] The H1′-H2′ cross peaks were observed from the TOCSY spectra of C(1), **2**(8), and G(12) (Fig. 3). The H1′-H2′ cross peaks for C(1) and G(12) were attributed to the conformational equilibrium of the sugar pucker between C2′-*endo* and C3′-*endo* because the cross peaks are often observed for residues at the ends of the oligonucleotides. On the other hand, the observed H1′-H2′ cross peaks for **2**(8) in the middle of the oligonucleotide suggested that **2** prefers the C2′-*endo* conformation.

2.5. Circular dichroism (CD) spectra

The global conformations of siRNAs are important for their RNAi activity. The human immunodeficiency virus (HIV)-1 transactivating response (TAR) RNA-binding protein (TRBP) has been reported to bind A-form duplexes but not B-form duplexes.[35] Thus, the CD spectra of siRNAs with and without modifications (siRNA **1**, siRNA **2**, siRNA **3** and siRNA **4**) were measured. As shown in Fig. 4, siRNAs exhibited positive CD bands at around 270 nm and negative bands at 210 nm, which were characteristic of an A-type duplex. However, the CD bands around 270 nm were slightly more shifted to red as the side chains of the modified siRNAs became longer. These results suggested that although the modified siRNAs formed A-type duplexes, incorporation of 4′-*C*-aminoalkyl modifications induced slight conformational changes in the siRNA duplexes.

2.6. Molecular modeling study

Thermal denaturation study, NMR measurements, and CD spectra suggested that 4′-*C*-aminoalkyl-2′-*O*-methyl modifications caused conformational changes in the dsRNA. Therefore, to determine the effects of 4′-*C*-aminoalkyl-2′-*O*-methyl modifications on sugar puckering, we calculated the percentage of 4′-*C*-aminoalkyl-2′-*O*-methyluridines **1**, **2** and **3** in the C3′-*endo* sugar conformation based on 100-ns MD trajectories (Fig. S5 and Table 4). During MD simulation, sugar conformations at each nucleotide were determined based on the pseudo rotational angles.[36] A previous study showed that the 4′-*C*-aminomethyl-2′-*O*-methyl modification nucleotide drove the sugar conformation to the south-type C2′-*endo* pucker. Similar results were observed for the 4′-*C*-aminoethyl-2′-*O*-methyl and 4′-*C*-aminopropyl-2′-*O*-methyl modifications. Longer side chain lengths resulted in a higher percentage of the population in the C2′-*endo* sugar conformation. Therefore, longer side chains induced greater conformational changes in the dsRNA. These results indicated that 4′-*C*-aminoalkyl modification of dsRNA caused the conformational changes, such as sugar puckering, which in turn resulted in the unfavorable entropy changes in the dsRNAs.

2.7. RNAi activity

The RNAi activities of the modified and unmodified siRNAs were assessed via dual luciferase reporter assays using a vector encoding *Renilla* and firefly luciferases in HeLa cells. The siRNAs targeting the *Renilla* luciferase gene were transfected using RNAiMAX. After 24 h, the expression levels of both luciferase genes were analyzed. The relative percentage of *Renilla*: firefly luciferase activity with respect to the no siRNA control is shown in Tables S2–S7 and Figs. 5–8.

Most siRNAs (siRNA **6–29**), which contained one analog at the passenger strand, effectively downregulated the expression of the *Renilla* luciferase gene both at 1 and 10 nM concentrations, which is similar to the effects observed with the unmodified siRNA (siRNA **5**) (Fig. 5). Slight reduction in RNAi activity was observed only when siRNA containing the analog with an aminopropyl group at position 11 from the 5′-end (siRNA **21**) was used at a concentration of 1 nM, suggesting that the 4′-*C*-aminopropyl modification located near the cleavage site slightly influences recognition by Ago2.[37] Furthermore, we examined the RNAi activity of siRNAs (siRNA **30–38**), which contained three analogs at the 5′-, middle, or 3′-regions of the passenger strand. As

Table 1
Sequences of ssRNAs, dsRNAs, and T_m values of dsRNAs.

Abbreviation of dsRNA	Abbreviation of ssRNA	Sequence[a]	T_m (°C)	ΔT_m (°C)[b]	ΔT_m (°C)/mod.
dsRNA **1**	RNA **1** RNA **9**	**F**-5′-UUCUUCUUCUU-3′-S 3′-AAGAAGAAGAA-5′	43.5 (± 0.1)	–	–
dsRNA **2**	RNA **2** RNA **9**	**F**-5′-U**1**CUUC**1**UC**1**U-3′-S 3′-AAGAAGAAGAA-5′	37.6 (± 0.2)	−5.9 (± 0.3)	−2.0 (± 0.1)
dsRNA **3**	RNA **3** RNA **9**	**F**-5′-U**2**CUUC**2**UC**2**U-3′-S 3′-AAGAAGAAGAA-5′	37.3 (± 0.1)	−6.3 (± 0.1)	−2.1 (± 0.0)
dsRNA **4**	RNA **4** RNA **9**	**F**-5′-U**3**CUUC**3**UC**3**U-3′-S 3′-AAGAAGAAGAA-5′	36.6 (± 0.1)	−7.0 (± 0.1)	−2.3 (± 0.0)

The T_m values were determined using 3 μM dsRNA in a buffer containing 10 mM sodium phosphate (pH 7.0) and 100 mM NaCl.
[a] **F** denotes a fluorescein. S shows an ethynyl linker. [b]ΔT_m represents [T_m (dsRNA$_{mod}$) – T_m (dsRNA$_{unmod}$)].

Table 2
Sequences of ssRNAs, siRNAs, and T_m values of siRNAs.

Abbreviation of siRNA	Abbreviation of ssRNA	Sequence[a]	T_m (°C)	ΔT_m (°C)[b]	ΔT_m (°C)/mod.
siRNA **1**	RNA **13** RNA **14**	5′-GGCCUUUCACUACUCCUACUU-3′ 3′-UUCCGGAAAGUGAUGAGGAUG-5′-**F**	79.5 (± 0.4)	–	–
siRNA **2**	RNA **15** RNA **16**	5′-GGCC**111**CAC**1**AC**1**CC**1**AC**11**-3′ 3′-**11**CCGGAAAG**1**GA**1**GAGGA**1**G-5′-**F**	65.7 (± 0.6)	−13.7 (± 0.4)	−1.06 (± 0.03)
siRNA **3**	RNA **17** RNA **18**	5′-GGCC**222**CAC**2**AC**2**CC**2**AC**22**-3′ 3′-**22**CCGGAAAG**2**GA**2**GAGGA**2**G-5′-**F**	65.0 (± 0.6)	−14.6 (± 0.2)	−1.11 (± 0.01)
siRNA **4**	RNA **19** RNA **20**	5′-GGCC**333**CAC**3**AC**3**CC**3**AC**33**-3′ 3′-**33**CCGGAAAG**3**GA**3**GAGGA**3**G-5′-**F**	64.6 (± 0.2)	−14.8 (± 0.3)	−1.16 (± 0.04)

The T_m values were determined using 3 μM dsRNA in a buffer containing 10 mM sodium phosphate (pH 7.0) and 100 mM NaCl.
[a] **F** denotes a fluorescein. [b]ΔT_m represents [T_m (siRNA$_{mod}$) – T_m (siRNA$_{unmod}$)].

shown in Fig. 6, although slight decrease in RNAi activities was observed at 1 nM, siRNAs harboring three modifications at the passenger strand still preserved their RNAi activities.

As passenger strand modification at one or three positions did not affect RNAi activity, we next examined the RNAi activities of siRNAs harboring eight analogs in the passenger strand (siRNA **39**–**41**). As shown in Fig. 7, the RNAi activities of 1 nM siRNAs were lower than those of the unmodified siRNAs. Longer aminoalkyl groups tended to show reduced RNAi activities. The minor groove of the siRNA was crowded with the aminoalkyl groups when the eight analogs were introduced into the siRNA. Thus, steric hindrance by the aminoalkyl groups might interfere with RISC formation.[38,39] Furthermore, as the 4′-*C*-aminoalkyl modification shifts the sugar conformation of the nucleoside from C3′-endo to C2′-*endo* puckering, this conformational change might influence Ago2 recognition. However, notably, siRNAs harboring the eight analogs showed sufficient RNAi activities at 10 nM.

Finally, the modifications were introduced into the guide strand of siRNAs (siRNA **42**–**50**) (Fig. 8). The region spanning nucleoside positions 2–8 from the 5′-end of the guide strand is referred to as the seed region. It is known that the formation of base pairs between the siRNA and target mRNA in this region is crucial for eliciting the RNAi activity of the siRNA.[38] It was reported that incorporation of 4′-*C*-aminomethyl-2′-*O*-methyluridine (**1**) at the seed region inhibited the RNAi activity of the siRNA.[25] Similarly, incorporation of 4′-*C*-aminoethyl-2′-*O*-methyluridine (**2**) or 4′-*C*-aminopropyl-2′-*O*-methyluridine (**3**) at the nucleoside position 2 from the 5′-end (siRNA **49** and **50**) was detrimental to RNAi activity. However, surprisingly, the aminoalkyl modifications at nucleoside position 8 from the 5′-end (siRNA **45**–**47**) did not affect RNAi activity although this position is within the seed region. Furthermore, aminoalkyl modifications in the guide strand outside the seed region (siRNA **42**–**44**) did not abolish RNAi activity, although 1 nM aminopropyl modification slightly reduced RNAi activity. These results suggested that the 4′-*C*-aminoalkyl modifications at the passenger strand and the guide strand outside the seed region did not significantly affect Ago2 recognition, although Ago2 recognizes the minor groove of siRNA.

2.8. Stability in serum

Natural RNA oligomers are easily degraded by nucleases that are present both inside and outside of cells and thus limit the application of RNA drugs. Therefore, chemical modifications are required to increase the half-life of siRNAs and prevent nucleolytic degradation by these nucleases. The 4′-*C*-aminoalkyl modifications are expected to enhance the stability of the RNA oligomers. Thus, we assessed the effects of 4′-*C*-aminoalkyl modifications on the stabilities of ssRNAs (RNA **1**–**4**) and siRNAs (siRNA **1**–**4**) in serum. First, 11-mer RNA labeled at the 5′-end with fluorescein was incubated in buffer containing 3% bovine serum and subsequently analyzed via PAGE. As shown in Fig. 9, the unmodified RNA was degraded by nucleases in serum within 1 h of incubation. On the other hand, the modified RNAs exhibited considerably longer half-lives than those of native RNA. The half-lives of RNA **1**, RNA **2**, RNA **3**, and RNA **4** were determined to be 0.05, 2.1, 15 and 32 h, respectively. Although the RNA harboring the 4′-*C*-aminomethyl-2′-*O*-methyluridine modification exhibited longer half-life than the native RNA, most of the full-length RNA was degraded after 6 h of incubation. On the other hand, full length RNAs containing 4′-*C*-aminoethyl-2′-*O*-methyl and 4′-*O*-aminopropyl-2′-*O*-methyl modifications were still intact even after 6 h of incubation. We hypothesized that the ammonium cations, which were produced via protonation of the terminal amino functions of the aminoalkyl groups, interacted with the active centers of the nucleases in the serum and inhibited the hydrolysis of the RNAs. These results suggested that the ammonium cations of flexible and long chains can effectively interact with nucleases and inhibit their activities.

Next, we examined the stabilities of the modified siRNAs in serum. The modified and unmodified siRNAs, which were fluorescein-labeled at the 5′-ends of the guide strands, were incubated in buffer containing 10% bovine serum. As shown in Fig. 10, the modified siRNAs showed high stability in serum than the single-stranded RNAs. The unmodified siRNAs were degraded by nucleases in serum within 3 h of incubation, whereas the modified siRNAs remained intact after 6 h.

Table 3
Thermodynamic parameters of the dsRNAs.

Abbreviation of dsRNA	Abbreviation of ssRNA	Sequence	ΔH° (kcal/mol)	ΔS° (cal/mol·K)	$\Delta G^\circ_{37°C}$ (kcal/mol)
dsRNA **5**	RNA **5** RNA **9**	5′-UUCUUCUUCUU-3′ 3′-AAGAAGAAGAA-5′	−86.8	−245.7	−10.6
dsRNA **9**	RNA **6** RNA **9**	5′-UUCUUC**1**UCUU-3′ 3′-AAGAAGAAGAA-5′	−91.2	−261.8	−10.1
dsRNA **13**	RNA **7** RNA **9**	5′-UUCUUC**2**UCUU-3′ 3′-AAGAAGAAGAA-5′	−92.5	−266.1	−10.0
dsRNA **17**	RNA **8** RNA **9**	5′-UUCUUC**3**UCUU-3′ 3′-AAGAAGAAGAA-5′	−94.2	−272.2	−9.8

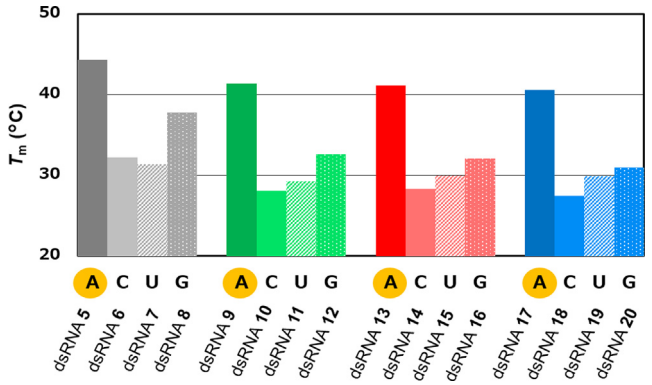

Fig. 2. Base-discriminating abilities of RNAs containing 4′-*C*-aminoalkylnucleoside analogs. Gray: unmodified dsRNAs. Green: dsRNAs containing the aminomethyl analog **1**. Red: dsRNAs containing the aminoethyl analog **2**. Blue: dsRNAs containing the aminopropyl analog **3**.

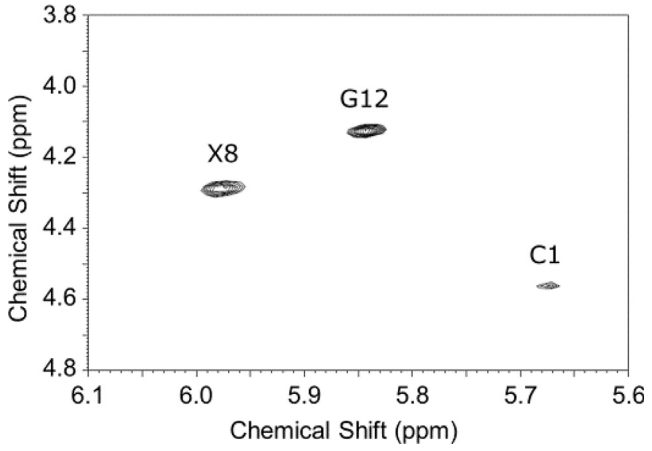

Fig. 3. TOCSY spectra of 5′-CGCGAAU**2**CGCG-3′ at the 3.8–4.8 ppm and 5.6–6.1 ppm regions in D_2O at 45 °C.

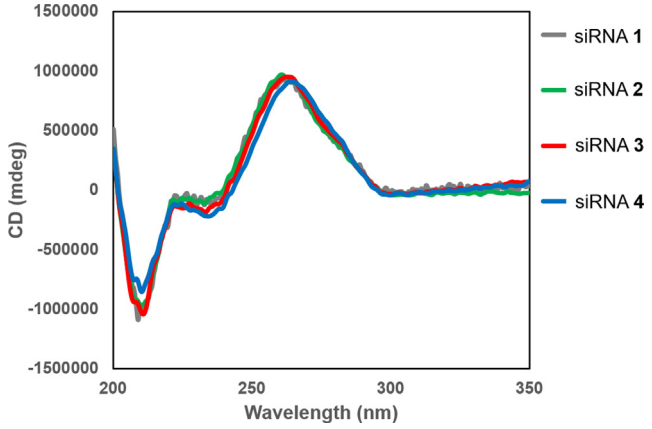

Fig. 4. CD spectra of the modified and unmodified siRNAs in a buffer containing 10 mM sodium phosphate (pH 7.0) and 0.1 M NaCl at 15 °C. The concentration of duplexes was 4 μM.

3. Conclusions

In the present study, we successfully demonstrated the synthesis of 4′-*C*-aminoethyl-2′-*O*-methyluridine (**2**) and 4′-*C*-aminopropyl-2′-*O*-methyluridine (**3**) and the oligonucleotides (ONs) containing the analogs. Incorporation of the analogs into dsRNAs and siRNAs decreased the T_m values of dsRNAs and siRNAs by 1–2 °C/modification. However,

Table 4
Ratio of C3′-*endo* puckering of the unmodified and modified uridine.

	C3′-*endo* (%)
Uridine	38.5
2	16.4
3	16.1

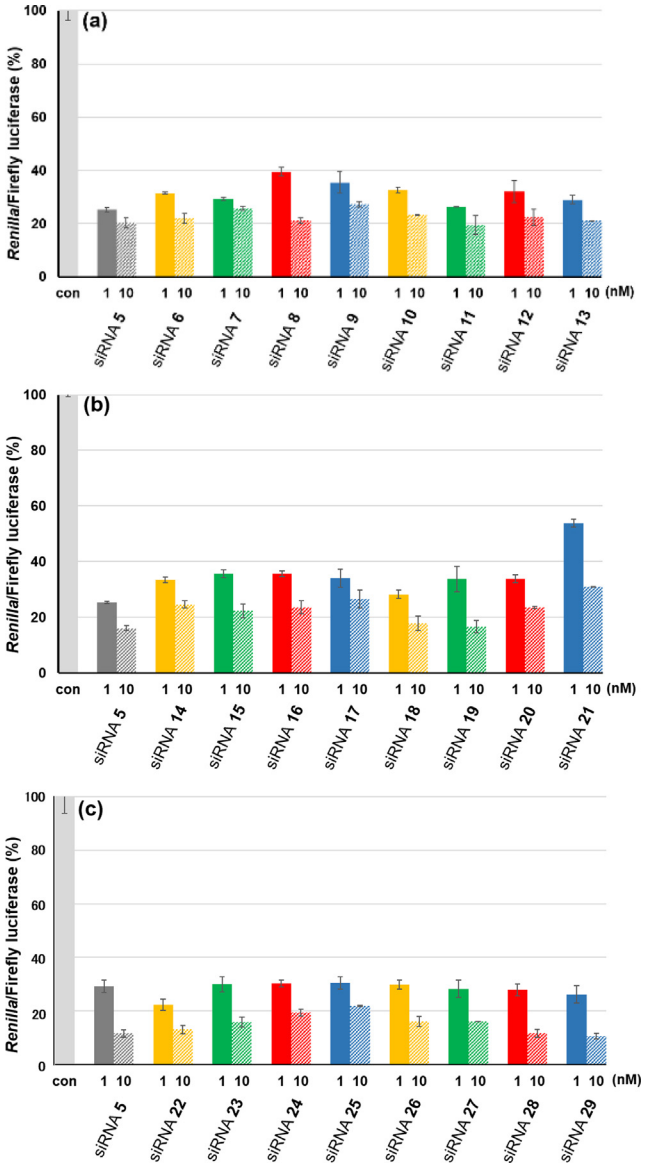

Fig. 5. RNAi activities of siRNAs modified by one analog at the passenger strands. Experimental conditions are described in the experimental section.

the T_m values of the siRNAs were around 60 °C, it was found that the siRNAs with the 4′-*C*-aminoalkyl modifications could form stable duplexes under biological conditions. On the other hand, the 4′-*C*-aminoalkyl modifications significantly increased the nuclease resistance of the single-stranded RNAs (ssRNAs) and siRNAs. Furthermore, the 4′-*C*-aminoalkyl modifications at the passenger strand and the guide strand outside the seed region were well tolerated for RNAi activities. Thus, siRNAs containing the 4′-*C*-aminoethyl and 4′-*C*-aminopropyl analogs are good candidates for the development of therapeutic siRNA molecules.

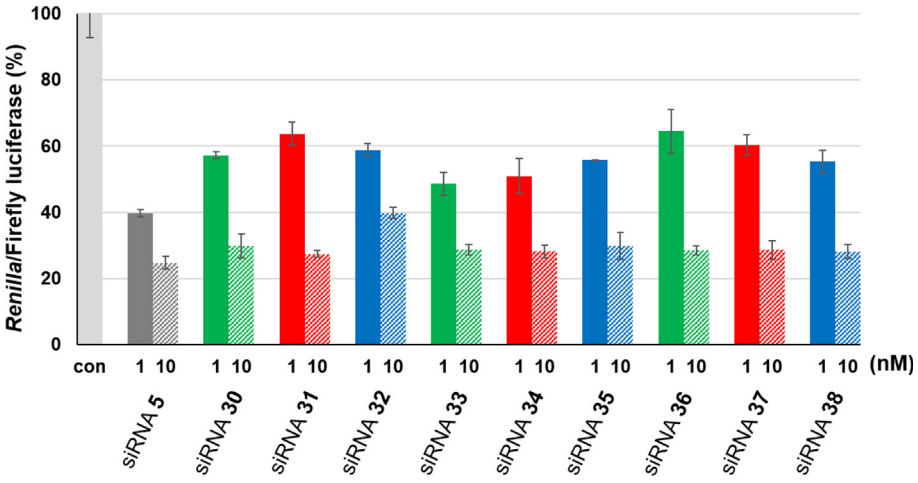

Fig. 6. RNAi activities of siRNAs modified by three analogs at the passenger strands. Experimental conditions are described in the experimental section.

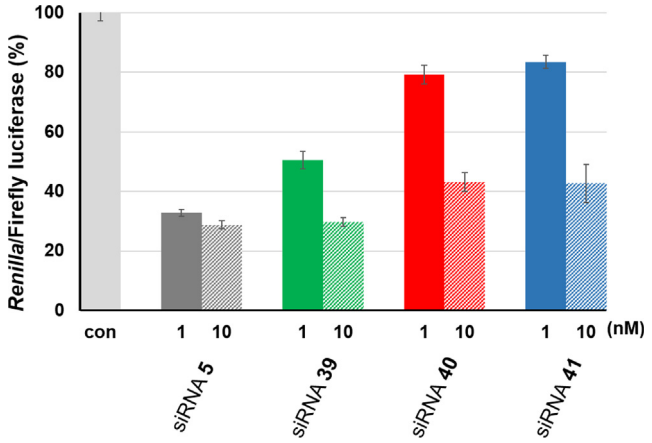

Fig. 7. RNAi activities of siRNAs modified by eight analogs at the passenger strands. Experimental conditions are described in the experimental section.

4. Experimental section

4.1. General remarks

$CDCl_3$ or DMSO-d_6 was used as a solvent for obtaining NMR spectra. Chemical shifts (δ) are given in parts per million (ppm) downfield from $(CH_3)_4Si$ ($\delta = 0.00$ for ^1H NMR in $CDCl_3$), or a solvent (for ^{13}C NMR and ^1H NMR in DMSO-d_6) as an internal standard for coupling constants (J) in Hz. The abbreviations s, d, q and m signify singlet, doublet, quadruplet and multiplet, respectively.

4.2. 5-O-[(1,1-Dimethylethyl)diphenylsilyl]-4-C-vinyl-3-O-benzyl-1,2-O-isopropylidene-α-D-ribofuranose (5)

Sodium hydride (NaH, 60% in mineral, 2.24 g, 56.0 mmol) was added to DMSO (40 mL) under argon atmosphere and mixture was stirred for 30 min at 80 °C. after the mixture was cooled down to room temperature, a solution of methyltriphenylphosphonium bromide (Ph_3PMeBr, 20.0 g, 56.0 mmol) in anhydrous DMSO (60 mL) was added dropwise to the mixture at 0 °C and the mixture was stirred for 30 min at room temperature. A solution of **4** (23.5 g, 42.5 mmol) in anhydrous DMSO (100 mL) was added dropwise and the mixture was stirred for 3.5 h at room temperature. The mixture was poured into H_2O in an ice-bath and extracted with EtOAc. The organic layer was washed with brine, dried over Na_2SO_4 and concentrated in vacuo. The residue was purified by chromatography on silica gel (hexane/EtOAc = 10:1) to give **5** as a colorless oil (16.6 g, 30.4 mmol, 72%). ^1H NMR (600 MHz, $CDCl_3$) δ 1.00 (s, 9H), 1.32 (s, 6H), 3.52 (dd, J = 11.7 Hz and 7.6 Hz, 2H), 4.46 (d, J = 4.8 Hz, 1H), 4.64–4.68 (m, 2H), 4.83 (d, J = 12.4 Hz, 1H), 5.19 (dd, J = 9.6 Hz and 2.0 Hz, 1H), 5.45 (d, J = 15.1 Hz, 1H), 5.81 (d, J = 4.1 Hz, 1H), 6.15–6.19 (m, 1H), 7.28–7.50 (m, 11H),

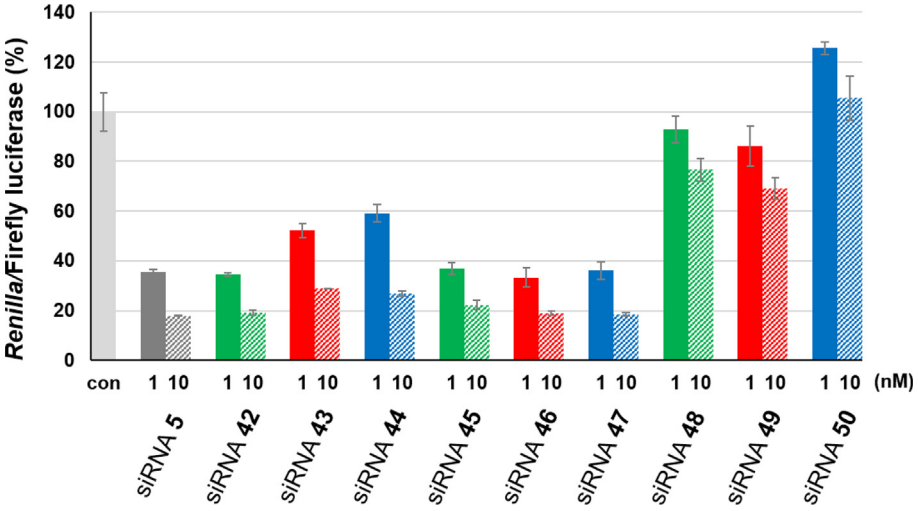

Fig. 8. RNAi activities of siRNAs modified by one analog at the guaide strands. Experimental conditions are described in the experimental section.

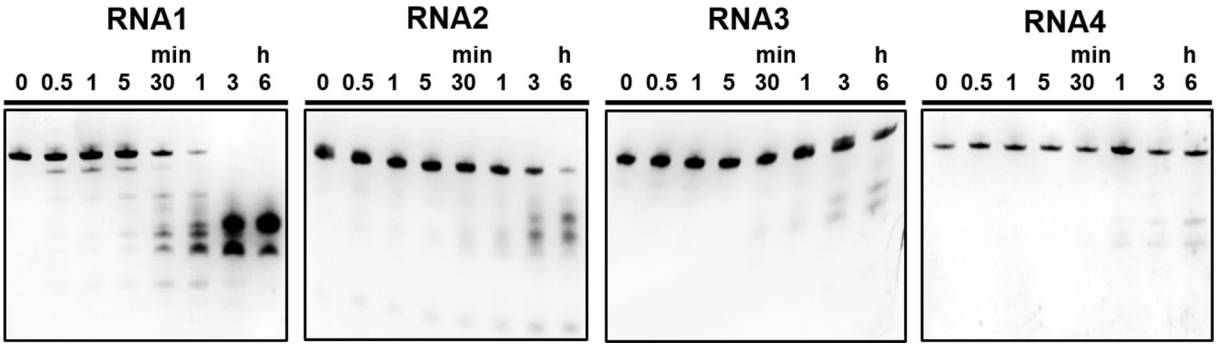

Fig. 9. PAGE of ssRNAs treated in buffer containing 3% bovine serum. Experimental conditions are described in the experimental section.

7.59–7.65 (m, 4H). ^{13}C NMR (101 MHz, $CDCl_3$) δ 19.4, 26.0, 26.4, 26.9, 66.5, 72.6, 77.0, 77.1, 77.4, 78.9, 87.5, 104.1, 113.6, 116.4, 127.8, 127.8, 127.9, 128.0, 128.6, 129.8, 129.8, 133.1, 133.6, 135.7, 135.8, 138.1. HRMS (ESI-TOF) *m/z* Calcd for $C_{33}H_{40}KO_5Si$ $[M+Na]^+$ 583.2282, Found 583.2292.

*4.3. 5-O-[(1,1-Dimethylethyl)diphenylsilyl]-4-C-hydroxyethyl-3-O-benzyl-1,2-O-isopropylidene-α-D-ribofuranose (**6**)*

A 0.5 M in THF solution of 9-borabicyclo[3.3.1]nonane (9-BBN, 182 mL, 90.8 mmol) was added dropwise to a solution of **5** (16.6 g, 30.4 mmol) in anhydrous THF (100 mL) under argon atmosphere and the mixture was stirring for 13.5 h at room temperature·H_2O was added to the reaction until evolution of gas ceased. 3 N NaOH solution (60 mL) was added and then slowly 30% aqueous hydrogen peroxide solution (30 mL) was added while keeping the temperature between 30 and 50 °C. The mixture was stirred for 3 h and extracted with H_2O and EtOAc. The organic layer was washed with neutral phosphate buffer solution and brine, dried over Na_2SO_4 and concentrated in vacuo. The residue was purified by chromatography on silica gel (hexane/EtOAc = 10:1) to give 5 as a colorless oil (14.9 g, 26.4 mmol, 87%). ^{1}H NMR (400 MHz, $CDCl_3$) δ 0.99 (s, 9H), 1.36 (s, 3H), 1.68 (s, 3H), 1.71–1.72 (m, 1H), 2.43–2.48 (m, 1H), 2.80–2.82 (m, 1H), 3.42 (d, J = 11.0 Hz, 1H), 3.63–3.72 (m, 2H), 3.73 (d, J = 11.0 Hz, 1H), 4.29 (d, J = 5.5 Hz, 1H), 4.56 (d, J = 12.4 Hz, 1H), 4.68–4.70 (m, 1H), 4.81 (d, J = 11.9 Hz, 1H), 5.80 (d, J = 4.12 Hz, 1H), 7.30–7.45 (m, 11H), 7.57–7.64 (m, 4H). ^{13}C NMR (101 MHz, $CDCl_3$) δ 19.4, 22.9, 26.3, 26.6, 27.0, 27.3, 33.7, 35.0, 59.0, 66.9, 72.6, 78.0, 79.4, 88.4, 104.5, 113.9, 127.9, 127.9, 128.1, 128.6, 129.9, 130.0, 133.0, 133.2, 135.7, 135.8, 137.8. HRMS (ESI-TOF) *m/z* Calcd for $C_{33}H_{42}KO_6Si$ $[M+Na]^+$ 601.2388, Found 601.2395.

*4.4. 5-O-[(1,1-Dimethylethyl)diphenylsilyl]-4-C-(p-toluenesulfonyloxyethyl)-3-O-benzyl-1,2-O-isopropylidene-α-D-ribofuranose (**7a**)*

Pyridine (12.9 mL, 160 mmol) and *p*-toluenesulfonyl chloride (TsCl, 15.3 g, 80.0 mmol) was added to the solution of **6** (13.1 g, 23.3 mmol) in anhydrous CH_2Cl_2 (120 mL) under argon atmosphere at 0 °C and the mixture was stirred for 20 h at room temperature. The mixture was extracted with saturated $NaHCO_3$ solution and CH_2Cl_2. The organic layer was washed with brine, dried over Na_2SO_4 and concentrated in vacuo. The residue was purified by chromatography on silica gel (hexane/EtOAc = 4:1) to give **7a** as a colorless oil (13.5 g, 18.9 mmol, 81%). ^{1}H NMR (500 MHz, $CDCl_3$) δ 0.98 (s, 9H), 1.31 (s, 3H), 1.47 (s, 3H), 1.85–1.93 (m, 1H), 2.38 (s, 3H), 2.51–2.54 (m, 1H), 3.35 (d, J = 10.9 Hz, 1H), 3.58 (d, J = 10.9 Hz, 1H), 4.11–4.18 (m, 1H), 4.20 (d, J = 5.8 Hz, 1H), 4.26–4.31 (m, 1H), 4.49 (d, J = 12.0 Hz, 1H), 4.59–4.62 (m, 1H), 4.74 (d, J = 12.0 Hz, 1H), 5.71 (d, J = 4.00 Hz, 1H), 7.19 (d, J = 8.0 Hz, 2H), 7.28–7.45 (m, 11H), 7.55–7.64 (m, 6H). ^{13}C NMR (101 MHz, $CDCl_3$) δ 19.3, 21.7, 26.2, 26.7, 26.9, 31.3, 67.1, 67.6, 72.5, 78.0, 79.1, 86.4, 104.5, 113.4, 127.8, 127.9, 127.9, 127.9, 128.0, 128.6, 129.8, 132.0, 133.2, 133.4, 135.7, 135.7, 137.8, 144.4. HRMS (ESI-TOF) *m/z* Calcd for $C_{40}H_{48}NaO_8SSi$ $[M+Na]^+$ 739.2737, Found 739.2746.

*4.5. 5-O-[(1,1-Dimethylethyl)diphenylsilyl]-4-C-(p-toluenesulfonyloxyethyl)-3-O-benzyl-1,2-di-O-acetyl-α-D-ribofuranose (**8**)*

Acetic anhydride (Ac_2O, 17.5 mL, 189 mmol) and 1% H_2SO_4 in AcOH (5.1 mL) was added to a solution of **7a** (13.5 g, 18.9 mmol) in AcOH (40 mL) at 0 °C and the mixture was stirred for 30 min at room temperature. The mixture was extracted with H_2O and EtOAc. The organic layer was washed with saturated $NaHCO_3$ solution and brine, dried over Na_2SO_4 and concentrated in vacuo. The residue was purified by chromatography on silica gel (hexane/EtOAc = 4:1) to give **8** as a colorless oil (13.0 g, 17.1 mmol, 90%). ^{1}H NMR (500 MHz, $CDCl_3$) δ 1.02 (s, 9H), 1.75 (s, 3H), 2.03 (s, 3H), 2.06–2.15 (m, 1H), 2.24–2.36 (m, 1H), 2.39 (s, 3H), 3.47–3.52 (m, 2H), 4.15–4.20 (m, 1H), 4.25 (d, J = 5.2 Hz, 1H), 4.28–4.33 (m, 1H), 4.48 (d, J = 10.9 Hz, 1H), 4.54 (d, J = 10.9 Hz, 1H), 5.29 (d, J = 5.2 Hz, 1H), 6.04 (s, 1H), 7.22–7.24 (m, 4H), 7.30–7.48 (m, 10H), 7.58–7.72 (m, 5H). ^{13}C NMR (126 MHz, $CDCl_3$) δ 19.4, 20.8, 21.0, 21.7, 27.0, 31.1, 67.6, 67.5, 73.6, 74.3, 79.1, 86.8, 97.7, 127.6, 127.9, 128.0, 128.6, 129.9, 130.0, 130.1, 132.7,

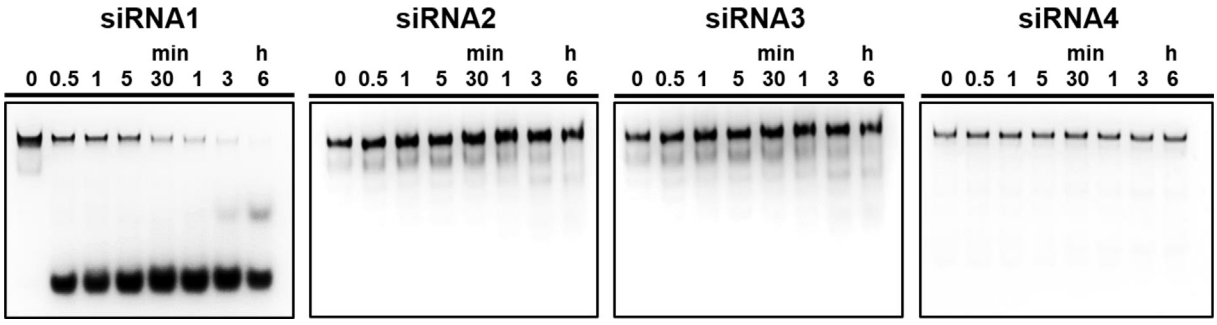

Fig. 10. PAGE of siRNAs treated in buffer containing 10% bovine serum. Experimental conditions are described in the experimental section.

133.1, 133.4, 135.6, 135.7, 137.3, 144.5. HRMS (ESI-TOF) *m/z* Calcd for $C_{41}H_{48}KO_{10}SSi$ $[M+Na]^+$ 799.2375, Found 799.2395.

4.6. 5-O-[(1,1-Dimethylethyl)diphenylsilyl]-4-C-azidoethyl-3-O-benzyl-1,2-di-O-acetyl-α-D-ribofuranose (9a)

NaN_3 (1.04 g, 16.0 mmol) was added to a solution of **8** (3.48 g, 4.57 mmol) in DMF (35 mL) under argon atmosphere and the mixture was stirred overnight at 50 °C. The mixture was extracted with brine and EtOAc. The organic layer was washed with brine, dried over Na_2SO_4 and concentrated in vacuo. The residue was purified by chromatography on silica gel (hexane/EtOAc = 7:1) to give **9a** as a colorless oil (2.37 g, 3.75 mmol, 82%). ^{1}H NMR (400 MHz, $CDCl_3$) δ 1.07 (s, 9H), 1.81 (s, 3H), 1.97–2.05 (m, 1H), 2.10 (s, 3H), 2.14–2.21 (m, 1H), 3.25–3.31 (m, 1H), 3.39–3.46 (m, 1H), 3.60 (s, 2H), 4.32 (d, J = 5.0 Hz, 1H), 4.52 (d, J = 11.5 Hz, 1H), 4.59 (d, J = 11.4 Hz, 1H), 5.35 (d, J = 5.0 Hz, 1H), 6.14 (s, 1H), 7.27–7.46 (m, 10*H*), 7.62–7.65 (m, 5H). ^{13}C NMR (151 MHz, $CDCl_3$) δ 19.5, 21.0, 21.1, 27.0, 31.6, 46.8, 68.0, 73.7, 74.6, 79.3, 87.1, 97.8, 127.6, 127.9, 128.0, 128.1, 128.6, 130.0, 130.1, 132.7, 133.1, 135.7, 135.8, 137.5, 169.3, 169.8. HRMS (ESI-TOF) *m/z* Calcd for $C_{34}H_{41}N_3NaO_7Si$ $[M+Na]^+$ 654.2612, Found 654.2632.

4.7. 5′-O-[(1,1-Dimethylethyl)diphenylsilyl]-4′-C-azidoethyl-3′-O-benzyl-2′-O-acetyluridine (10a)

Uracil (3.95 g, 35.2 mmol) and *N,O*-bis(trimethylsilyl)acetamide (BSA, 34.4 mL, 141 mmol) was added to a solution of **9a** (11.1 g, 17.6 mmol) in MeCN (100 mL) under argon atmosphere and the mixture was stirred 1 h at 95 °C. The mixture was cooled to room temperature, trimethylsilyl trifluoromethanesulfonate (TMSOTf, 6.36 mL, 35.2 mmol) was added dropwise to the mixture at 0 °C and the mixture was stirred for 3 h at 50 °C. Saturated $NaHCO_3$ solution was added to the mixture at 0 °C. The mixture was extracted with saturated $NaHCO_3$ solution and $CHCl_3$. The organic layer was washed with saturated $NaHCO_3$ solution, dried over Na_2SO_4 and concentrated in vacuo. The residue was purified by chromatography on silica gel (hexane/EtOAc = 2:1) to give **10a** as a white solid (10.2 g, 14.9 mmol, 85%). ^{1}H NMR (400 MHz, $CDCl_3$) δ 1.10 (s, 9H), 1.65–1.73 (m, 1H), 2.05–2.14 (m, 4H), 3.23–3.30 (m, 1H), 3.35–3.41 (m, 1H), 3.56 (d, J = 11.5 Hz, 1H), 3.86 (d, J = 11.5 Hz, 1H), 4.39–4.42 (m, 2H), 4.61 (d, J = 11.0 Hz, 1H), 5.32–5.39 (m, 2H), 6.13 (d, J = 5.04 Hz, 1H), 7.33–7.49 (m, 10H), 7.57–7.64 (m, 6H), 8.02 (s, 1H). ^{13}C NMR (151 MHz, $CDCl_3$) δ 19.5, 20.9, 27.18, 3.09, 46.5, 66.5, 74.6, 74.9, 86.9, 87.4, 103.1, 128.0, 128.2, 128.3, 128.4, 128.7, 130.4, 130.5, 131.9, 132.6, 135.5, 135.8, 137.1, 139.9, 150.2, 162.8, 170.1. HRMS (ESI-TOF) *m/z* Calcd for $C_{36}H_{41}N_5NaO_7Si$ $[M+Na]^+$ 706.2673, Found 706.2676.

4.8. 5′-O-[(1,1-Dimethylethyl)diphenylsilyl]-4′-C-azidoethyl-3′-O-benzyluridine (11a)

NH_3 solution (83 mL) was added to a solution of **10a** (10.2 g, 14.9 mmol) in MeOH (83 mL) and the mixture was stirred overnight at room temperature. The mixture was concentrated in vacuo. The residue was purified by chromatography on silica gel (hexane/EtOAc = 1:1) to give **11a** as a white solid (9.39 g, 14.6 mmol, 98%). ^{1}H NMR (500 MHz, $CDCl_3$) δ 1.09 (s, 9H), 1.67–1.73 (m, 1H), 2.15–2.21 (m, 1H), 3.20–3.26 (m, 1H), 3.33–3.38 (m, 1H), 3.47–3.55 (m, 2H), 3.80 (d, J = 10.9 Hz, 1H), 4.19 (d, J = 6.3 Hz, 1H), 4.30 (q, J = 5.8 Hz, 1H), 4.59 (d, J = 11.5 Hz, 1H), 4.72 (d, J = 11.5 Hz, 1H), 5.39 (d, J = 8.6 Hz, 1H), 5.90 (d, J = 5.7 Hz, 1H), 7.32–7.42 (m. 9H), 7.45–7.48 (m, 2H), 7.57–7.62 (m, 5H), 9.20 (s, 1H). ^{13}C NMR (151 MHz, $CDCl_3$) δ 19.4, 27.2, 31.2, 46.6, 66.9, 74.7, 75.0, 78.8, 87.2, 89.4, 102.8, 128.2, 128.3, 128.4, 128.6, 128.9, 130.4, 130.5, 132.0, 132.6, 135.5, 135.7, 136.9, 140.0, 150.8, 163.0. HRMS (ESI-TOF) *m/z* Calcd for $C_{34}H_{39}N_5NaO_6Si$ $[M+Na]^+$ 664.2567, Found 664.2547.

4.9. 5′-O-[(1,1-Dimethylethyl)diphenylsilyl]-4′-C-azidoethyl-3′-O-benzyl-2′-O-methyluridine (12a)

NaH (1.14 g, 28.4 mmol) was added to a solution of **11a** (6.06 g, 9.46 mmol) in THF (60 mL) at 0 °C under argon atmosphere and the mixture was stirred 10 min at 0 °C. Then methyl iodide (MeI, 2.94 mL, 47.3 mmol) was added dropwise to the mixture and stirred 8 h at 0 °C. Saturated $NaHCO_3$ solution was added to the mixture at 0 °C. The mixture was extracted with saturated $NaHCO_3$ solution and EtOAc. The organic layer was washed with brine, dried over Na_2SO_4 and concentrated in vacuo. The residue was purified by chromatography on silica gel (hexane/EtOAc = 2:1) to give **12a** as a white solid (4.18 g, 6.37 mmol, 67%). ^{1}H NMR (400 MHz, $CDCl_3$) δ 1.09 (s, 9H), 1.71–1.77 (m, 1H), 2.29–2.35 (m, 1H), 3.25–3.31 (m, 1H), 3.34–3.39 (m, 1H), 3.52 (s, 3H), 3.68 (d, J = 11.5 Hz, 1H), 3.75 (dd, J = 5.7 Hz and 2.3 Hz, 1H), 3.98 (d, J = 11.5 Hz, 1H), 4.35 (d, J = 6.3 Hz, 1H), 4.51 (d, J = 11.5 Hz, 1H), 4.71 (d, J = 11.5 Hz, 1H), 5.09 (dd, J = 8.0 Hz and 1.7 Hz, 1H), 6.08 (d, J = 2.3 Hz, 1H), 7.34–7.40 (m, 9H), 7.44–7.47 (m, 2H), 7.51 (d, J = 7.5 Hz, 2H), 7.61 (d, J = 6.9 Hz, 2H), 7.79 (d, J = 8.1 Hz, 1H), 8.96 (s, 1H). ^{13}C NMR (126 MHz, $CDCl_3$) δ 19.6, 27.3, 31.0, 46.6, 59.45, 65.5, 73.2, 75.8, 84.0, 87.3, 88.3, 102.6, 128.0, 128.2, 128.3, 128.3, 128.7, 130.3, 130.4, 132.0, 132.9, 135.4, 135.6, 137.3, 140.0, 150.0, 163.1. HRMS (ESI-TOF) *m/z* Calcd for $C_{35}H_{41}N_5NaO_6Si$ $[M+Na]^+$ 678.2724, Found 678.2704.

4.10. 5′-O-[(1,1-Dimethylethyl)diphenylsilyl]-4′-C-azidoethyl-2′-O-methyluridine (13a)

M of BCl_3 solution in CH_2Cl_2 (11.0 mL, 11.0 mmol) was added to a solution of **12a** (1.06 g, 1.62 mmol) in CH_2Cl_2 (42 mL) at −78 °C under argon atmosphere and the mixture was stirred for 3 h at −78 °C, then warmed to −30 °C and stirred 5 h. A solution of MeOH/CH_2Cl_2 (1:1, v/v) was added to the mixture. The mixture was concentrated in vacuo. The residue was purified by chromatography on silica gel (hexane/EtOAc = 1:1) to give **13a** as a white solid (0.713 g, 1.26 mmol, 78%). ^{1}H NMR (600 MHz, CDCl3) δ 1.11 (s, 9H), 1.73–1.78 (m, 1H), 2.05–2.10 (m, 1H), 2.89 (d, J = 5.5 Hz, 1H), 3.28–3.33 (m, 1H), 3.36–3.40 (m, 1H), 3.53 (s, 3H), 3.71 (d, J = 11.7 Hz, 1H), 3.89–3.93 (m, 2H), 4.49 (t, J = 6.2 Hz, 1H), 5.33 (d, J = 6.2 Hz, 1H), 6.08 (s, J = 4.1 Hz, 1H), 7.40–7.43 (m, 4H), 7.46–7.48 (m, 2H), 7.61 (d, J = 7.6 Hz, 2H), 7.65 (d, J = 7.6 Hz, 2H), 7.78 (d, J = 8.2 Hz, 1H), 9.11 (s, 1H). ^{13}C NMR (151 MHz, CDCl3) δ 19. 5, 27.2, 30.9, 46.6, 59.4, 66.8, 70.1, 84.4, 86.7, 87.8, 103.0, 128.2, 128.3, 130.4, 130.5, 131.8, 132.7, 135.4, 135.7, 139.9, 150.3, 163.4. HRMS (ESI-TOF) *m/z* Calcd for $_{28}H_{35}N_5NaO_6Si$ $[M+Na]^+$ 588.2254, Found 588.2266.

4.11. 4′-C-Azidoethyl-2′-O-methyluridine (14a)

1 M of tetrabutylammonium fluoride (TBAF) solution in THF (1.85 mL, 1.85 mmol) was added to a solution of **13a** (0.693 g, 1.23 mmol) in THF (7.0 mL) under argon atmosphere and the mixture was stirred for 21 h at room temperature. The mixture was concentrated in vacuo. The residue was purified by chromatography on silica gel ($CHCl_3$/MeOH = 8:1) to give **14a** as a white solid (0.390 g, 1.19 mmol, 97%). ^{1}H NMR (500 MHz, DMSO-d_6) δ 1.78–1.81 (m, 1H), 1.95–1.98 (m, 1H), 3.30 (s, 3H), 3.35–3.42 (m, 4H), 3.99 (t, J = 6.3 Hz, 1H), 4.18 (t, J = 5.8 Hz, 1H), 5.29–5.33 (m, 2H), 5.68 (d, J = 8.1 Hz, 1H), 5.92 (d, J = 6.9 Hz, 1H), 7.90 (d, 8.1 Hz, 1H), 11.4 (s, 1H). ^{13}C NMR (101 MHz, DMSO-d_6) δ 31.0, 46.4, 57.5, 64.3, 69.7, 82.3, 85.0, 87.2, 102.3, 140. 6, 150.7, 163.0. HRMS (ESI-TOF) *m/z* Calcd for $C_{12}H_{17}N_5O_6$ $[M+K]^+$ 366.0816, Found 366.0813.

4.12. 5′-O-[Bis(4-methoxyphenyl)phenylmethyl]-4′-C-azidoethyl-2′-O-methyluridine (15a)

4,4′-Dimethoxytrityl chloride (DMTrCl, 0.569 g, 1.68 mmol) was added to a solution of **14a** (0.365 g, 1.12 mmol) in pyridine (4.0 mL) under argon atmosphere and the mixture was stirred for 20 h at room temperature. The mixture was extracted with H_2O and EtOAc. The organic layer was washed with saturated $NaHCO_3$ solution and brine, dried over Na_2SO_4 and concentrated in vacuo. The residue was purified by chromatography on silica gel (hexane/EtOAc = 1:1) to give **15a** as a white solid (0.679 g, 1.08 mmol, 96%). ^{1}H NMR (400 MHz, $CDCl_3$) δ 1.74–1.81 (m, 1H), 2.08–2.11 (m, 1H), 2.87 (d, J = 6.4 Hz, 1H), 3.18–3.23 (m, 1H), 3.26–3.30 (m, 1H), 3.35 (s, 2H), 3.58 (s, 3H), 3.80 (s, 6H), 3.93 (dd, J = 6.0 Hz and 3.6 Hz, 1H), 4.10–4.15 (m, 1H), 4.61 (t, J = 6.4 Hz, 1H), 5.22 (d, J = 8.2 Hz, 1H), 6.03 (d, J = 3.6 Hz, 1H), 6.85 (d, J = 9.2 Hz, 4H), 7.24–7.25 (m, 2H), 7.26–7.35 (m, 7H), 7.81 (d, J = 8.2 Hz, 1H), 8.50 (s, 1H). ^{13}C NMR (151 MHz, $CDCl_3$) δ 31.2, 46.6, 55.4, 59.5, 65.4, 70.5, 84.5, 87.0, 87.2, 87.7, 102.7, 113.5, 123.4, 128.2, 128.3, 130.3, 130.4, 134.8, 135.0, 140.3, 144.2, 150.3, 158.9, 158.9, 163.2. HRMS (ESI-TOF) m/z Calcd for $C_{33}H_{35}N_5NaO_8$ $[M+Na]^+$ 652.2383, Found 652.2379.

4.13. 5′-O-[Bis(4-methoxyphenyl)phenylmethyl]-4′-C-trifluoroacetylaminoethyl-2′-O-methyluridine(17a)

Triphenylphosphine (PPh_3, 2.46 g, 9.38 mmol) and H_2O (2.70 mL) was added to a solution of **15a** (2.36 g, 3.75 mmol) in THF (100 mL) under argon atmosphere and the mixture was stirred for 18 h at 45 °C. The mixture was concentrated in vacuo. The residue was purified by chromatography on silica gel ($CHCl_3$/MeOH = 30:1) to give compound **16a**. CF_3CO_2Et (1.25 mL, 10.5 mmol) and Et_3N (0.728 mL, 5.25 mmol) were added to a solution of **16a** in CH_2Cl_2 (20 mL) and the mixture was stirred overnight at room temperature. The mixture was extracted with H_2O and EtOAc. The organic layer was washed with brine, dried over Na_2SO_4 and concentrated in vacuo. The residue was purified by chromatography on silica gel (hexane/EtOAc = 2:3) to give **17a** as a white solid (2.44 g, 3.49 mmol, 93%). ^{1}H NMR (600 MHz, $CDCl_3$) δ 1.92–1.94 (m, 1H), 2.00–2.05 (m, 1H), 3.09 (s, 1H), 3.27 (s, 1H), 3.31–3.40 (m, 3H), 3.53 (s, 3H), 3.80 (s, 6H), 4.03 (t, J = 4.8 Hz, 1H), 4.48 (s, 1H), 5.30 (d, J = 8.2 Hz, 1H), 6.06 (d, J = 4.8 Hz, 1H), 6.85 (d, J = 8.9 Hz, 4H), 7.13 (s, 1H), 7.23–7.25 (m, 4H), 7.29–7.35 (m, 5H), 7.69 (d, J = 8.3 Hz, 1H), 9.02 (s, 1H). ^{13}C NMR (151 MHz, $CDCl_3$) δ 31.0, 35.5, 55.4, 59.4, 65.9, 70.9, 83.9, 86.6, 87.7, 87.9, 103.0, 113.5, 127.6, 128.2, 128.3, 130.2, 130.3, 134.6, 134.8, 140.1, 144.0, 150.4, 159.0, 163.0. HRMS (ESI-TOF) m/z Calcd for $C_{35}H_{36}F_3N_3O_9$ $[M+Na]^+$ 722.2301, Found 722.2315.

4.14. 5′-O-[Bis(4-methoxyphenyl)phenylmethyl]-4′-C-trifluoroacetylaminoethyl-2′-O-methyl-3′-[2-cyanoethyl-N,N-bis(1-methylethyl)phosphoramidite]uridine (18a)

Chloro(2-cyanoethoxy)(*N,N*-diisopropylamino)phosphine (CEP-Cl, 0.638 mL, 2.86 mmol) and *N,N*-diisopropylethylamine (DIPEA. 1.25 mL, 7.15 mmol) were added to a solution of **17a** (1.00 g, 1.43 mmol) in THF (10 mL) under argon atmosphere and the mixture was stirred for 1.5 h at room temperature. The mixture was extracted with saturated $NaHCO_3$ solution and $CHCl_3$. The organic layer was washed with brine, dried over Na_2SO_4 and concentrated in vacuo. The residue was purified by chromatography on silica gel (hexane/EtOAc = 1:1) to give **18a** as a white solid (0.884 g, 0.983 mmol, 69%). ^{31}P NMR (162 MHz, $CDCl_3$) δ 150.94, 151.53. HRMS (ESI-TOF) m/z Calcd for $C_{44}H_{53}F_3N_5O_{10}P$ $[M+Na]^+$ 922.3380, Found 922.3371.

4.15. 5-O-[(1,1-Dimethylethyl)diphenylsilyl]-4-C-azidopropyl-3-O-benzyl-1,2-O-(1-methylethylidene)-α-D-ribofuranose (19)

NaN_3 (6.59 g, 12.1 mmol) was added to a solution of **7b** (8.82 g, 12.1 mmol) in DMF (90 mL) under argon atmosphere and the mixture was stirred overnight at 60 °C. The mixture was extracted with brine and EtOAc. The organic layer was washed with brine, dried over Na_2SO_4 and concentrated in vacuo. The residue was purified by chromatography on silica gel (hexane/EtOAc = 15:1) to give **19** as a colorless oil (5.98 g, 9.94 mmol, 82%). ^{1}H NMR (400 MHz, $CDCl_3$) δ 0.98 (s, 9H), 1.36 (s, 3H), 1.35–1.41 (m, 1H), 1.55–1.57 (m, 1H), 1.62 (s, 3H), 1.73–1.78 (m, 1H), 2.09–2.13 (m, 1H), 3.18–3.23 (m, 2H), 3.41 (d, J = 11.0 Hz), 3.65 (d, J = 11.0 Hz, 1H), 4.30 (d, J = 5.5 Hz, 1H), 4.59 (d, J = 12.4 Hz, 1H), 4.67 (dd, J = 5.5 Hz and 3.6 Hz, 1H), 4.82 (d, J = 12.4 Hz, 1H), 5.79 (d, J = 3.7 Hz, 1H), 7.30–7.46 (m, 10H), 7.59–7.64 (m, 5H). ^{13}C NMR (101 MHz, $CDCl_3$) δ 19.3, 23.3, 26.3, 26.9, 29.0, 52.2, 66.5, 72.6, 78.1, 79.5, 87.5, 104.3, 113.3, 127.8, 127.9, 128.6, 129.8, 129.9, 133.0, 133.3, 135.7, 135.8, 138.1. HRMS (ESI) m/z Calcd for $C_{34}H_{43}N_3O_5SiNa$ $[M+Na]^+$ 624.2870, found 624.2899.

4.16. 5-O-[(1,1-Dimethylethyl)diphenylsilyl]-4-C-azidopropyl-3-O-benzyl-1,2-di-O-acetyl-α-D-ribofuranose (9b)

A solution of **19** (0.40 g, 0.665 mmol) in 50% AcOH (5.70 mL) was warmed to 120 °C and stirred for 1 h. The mixture was concentrated in vacuo and dried by co-evaporation with EtOH. The residue was dissolved in pyridine (1.43 mL) and Ac_2O (0.95 mL, 10.2 mmol) was added under argon atmosphere. The mixture was stirred overnight at room temperature. The mixture was poured into H_2O in an ice-bath and extracted with EtOAc. The organic layer was washed with saturated $NaHCO_3$ solution and brine, dried over Na_2SO_4 and concentrated in vacuo. The residue was purified by chromatography on silica gel (hexane/EtOAc = 5:1) to give **9b** as a colorless oil (0.314 g, 0.486 mmol, 74%). ^{1}H NMR (400 MHz, $CDCl_3$) δ 1.06 (s, 9H), 1.10–1.14 (m, 1H), 1.54–1.58 (m, 1H), 1.74–1.77 (m, 1H), 1.82 (s, 3H), 1.84–1.90 (m, 1H), 2.10 (s, 3H), 3.19–3.23 (m, 2H), 3.59 (dd, J = 10.6 Hz and 13.3 Hz, 2H), 4.38 (d, J = 5.5 Hz, 1H), 4.54 (d, J = 11.4 Hz, 1H), 4.60 (d, J = 11.4 Hz, 1H), 5.36 (d, J = 5.5 Hz, 1H), 6.13 (s, 1H), 7.27–7.64 (m, 15H). ^{13}C NMR (101 MHz, $CDCl_3$) δ 19.5, 20.9, 22.9, 27.1, 29.5, 52.1, 67.4, 73.6, 74.9, 79.3, 88.1, 97.9, 127.6, 127.7, 127.9, 128.0, 130.1, 132.9, 133.2, 135.7, 135.8, 169.5, 169.9. HRMS (ESI) m/z Calcd for $C_{35}H_{43}N_3O_7SiNa$ $[M+Na]^+$ 668.2768, found 668.2747.

4.17. 5′-O-[(1,1-Dimethylethyl)diphenylsilyl]-4′-C-azidoepropyl-3′-O-benzyl-2′-O-acetyluridine (10b)

Uracil (0.957 g, 8.54 mmol) and BSA (11.1 mL, 34.2 mmol) was added to a solution of **9b** (2.76 g, 4.27 mmol) in MeCN (28 mL) under argon atmosphere and the mixture was stirred 1 h at 95 °C. The mixture was cooled to room temperature, TMSOTf (1.55 mL, 8.54 mmol) was added dropwise to the mixture at 0 °C and the mixture was stirred for 15 min at 95 °C. Saturated $NaHCO_3$ solution was added to the mixture at 0 °C. The mixture was extracted with saturated $NaHCO_3$ solution and $CHCl_3$. The organic layer was washed with saturated $NaHCO_3$ solution, dried over Na_2SO_4 and concentrated in vacuo. The residue was purified by chromatography on silica gel (hexane/EtOAc = 2:1) to give **10b** as a white solid (2.27 g, 3.26 mmol, 76%). ^{1}H NMR (400 MHz, $CDCl_3$) δ 1.09 (s, 9H), 1.45–1.51 (m, 2H), 1.64–1.69 (m, 1H), 1.82–1.89 (m, 1H), 2.11 (s, 3H), 3.18–3.24 (m, 2H), 3.56 (d, J = 11.4 Hz, 1H), 3.84 (d, J = 10.9 Hz, 1H), 4.39–4.44 (m, 2H), 4.61 (d, J = 11.0 Hz, 1H), 5.32–5.48 (m, 2H), 6.18 (d, J = 5.0 Hz, 1H), 7.28–7.57 (m, 15H), 7.67 (d, J = 8.2 Hz, 1H), 8.66 (s, 1H). ^{13}C NMR (101 MHz, $CDCl_3$) δ 19.5, 20.9, 23.0, 23.1, 27.0, 27.2, 29.2, 51.9, 66.5, 74.6, 75.1, 77.8, 86.3,

88.2, 103.0, 128.0, 128.1, 128.2, 128.3, 128.7, 130.3, 130.5, 132.0, 132.7, 135.5, 135.7, 135.78, 137.3, 139.8, 150.3, 162.8, 170.2. HRMS (ESI) *m/z* Calcd for $C_{37}H_{43}N_5O_7SiNa$ $[M+Na]^+$ 720.2829, found 720.2848.

4.18. 5′-O-[(1,1-Dimethylethyl)diphenylsilyl]-4′-C-azidopropyl-3′-O-benzyluridine (11b)

NH_3 solution (16 mL) was added to a solution of **10b** (1.57 g, 2.24 mmol) in MeOH (16 mL) and the mixture was stirred overnight at room temperature. The mixture was concentrated in vacuo. The residue was purified by chromatography on silica gel (hexane/EtOAc = 2:1) to give **11b** as a white solid (1.44 g, 2.19 mmol, 98%). ^{1}H NMR (400 MHz, $CDCl_3$) δ 1.09 (s, 9H), 1.37–1.41 (m, 1H), 1.51–1.55 (m, 1H), 1.61–1.68 (m, 1H), 1.85–1.89 (m, 1H), 3.13–3.19 (m, 2H), 3.55 (d, J = 11.0 Hz, 1H), 3.60 (d, J = 7.80 Hz, 1H), 3.78 (d, J = 11.0 Hz, 1H), 4.19 (d, J = 6.0 Hz, 1H), 4.29 (dd, J = 6.0 Hz and 12.4 Hz, 1H), 4.59 (d, J = 11.4 Hz, 1H), 4.74 (d, J = 11.5 Hz, 1H), 5.39 (d, J = 8.2 Hz, 1H), 5.94 (d, J = 5.5 Hz, 1H), 7.34–7.60 (m, 15H), 7.69 (d, J = 7.8 Hz, 1H), 9.37 (s, 1H). ^{13}C NMR (101 MHz, $CDCl_3$) δ 19.4, 23.0, 27.2, 29.4, 51.9, 66.8, 74.7, 75.2, 78.8, 87.9, 88.9, 102.8, 128.1, 128.2, 128.3, 128.5, 128.8, 130.3, 130.4, 132.1, 132.6, 135.5, 135.7, 137.1, 139.9, 151.0, 163.2. HRMS (ESI) *m/z* Calcd for $C_{35}H_{41}N_5O_6SiNa$ $[M+Na]^+$ 678.2724, found 678.2703.

4.19. 5′-O-[(1,1-Dimethylethyl)diphenylsilyl]-4′-C-azidopropyl-3′-O-benzyl-2′-O-methyluridine (12b)

NaH (60% in mineral, 0.972 g, 24.3 mmol) was added to a solution of **11b** (5.33 g, 8.10 mmol) in THF (53 mL) at 0 °C under argon atmosphere and the mixture was stirred 10 min at 0 °C. Then MeI (3.02 mL, 48.6 mmol) was added dropwise to the mixture and stirred 8 h at 0 °C. Saturated $NaHCO_3$ solution was added to the mixture at 0 °C. The mixture was extracted with saturated $NaHCO_3$ solution and EtOAc. The organic layer was washed with saturated $NaHCO_3$ solution and brine, dried over Na_2SO_4 and concentrated in vacuo. The residue was purified by chromatography on silica gel (hexane/EtOAc = 3:1) to give **12b** as a white solid (4.00 g, 5.98 mmol, 74%). ^{1}H NMR (400 MHz, $CDCl_3$) δ 1.08 (s, 9H), 1.39–1.46 (m, 1H), 1.52–1.60 (m, 1H), 1.65–1.70 (m, 1H), 1.97–2.05 (m, 1H), 3.19–3.26 (m, 2H), 3.51 (s, 3H), 3.68 (d, J = 11.5 Hz, 1H), 3.74 (m, 1H), 3.95 (d, J = 11.5 Hz, 1H), 4.35 (d, J = 4.6 Hz, 1H), 4.52 (d, J = 11.5 Hz, 1H), 4.73 (d, J = 11.9 Hz, 1H), 5.12 (d, J = 8.2 Hz, 1H), 6.09 (s, 1H), 7.35–7.63 (m, 15H), 7.78 (d, J = 8.2 Hz, 1H), 9.04 (s, 1H). ^{13}C NMR (101 MHz, $CDCl_3$) δ 19.6, 22.8, 27.3, 29.0, 51.8, 59.4, 65.4, 73.5, 75.9, 84.2, 87.9, 88.1, 102.6, 128.0, 128.1, 128.2, 128.3, 128.7, 130.3, 130.4, 132.1, 133.0, 135.4, 135.6, 137.5, 140.0, 150.1, 163.2. HRMS (ESI) *m/z* Calcd for $C_{36}H_{43}N_5O_6SiNa$ $[M+Na]^+$ 692.2880, found 692.2897.

4.20. 5′-O-[(1,1-Dimethylethyl)diphenylsilyl]-4′-C-azidopropyl-2′-O-methyluridine (13b)

1 M of BCl_3 solution in CH_2Cl_2 (35.9 mL, 35.9 mmol) was added to a solution of **12b** (4.00 g, 5.98 mmol) in CH_2Cl_2 (60 mL) at −78 °C under argon atmosphere and the mixture was stirred for 3 h at −78 °C, then warmed to −30 °C and stirred 5 h. A solution of MeOH/CH_2Cl_2 (1:1, v/v) was added to the mixture. The mixture was concentrated in vacuo. The residue was purified by chromatography on silica gel (hexane/EtOAc = 1:1) to give **13b** as a white solid (2.99 g, 5.16 mmol, 86%). ^{1}H NMR (600 MHz, $CDCl_3$) δ 1.11 (s, 9H), 1.49–1.56 (m, 2H), 1.58–1.64 (m, 1H), 1.76–1.80 (m, 1H), 2.74 (d, J = 5.5 Hz, 1H), 3.21–3.25 (m, 2H), 3.52 (s, 3H), 3.70 (d, J = 11.0 Hz, 1H), 3.88 (d, J = 11.0 Hz, 1H), 3.93 (m, 1H), 4.49 (t, J = 5.5 Hz, 1H), 5.31 (d, J = 8.3 Hz, 1H), 6.06 (d, J = 4.8 Hz, 1H), 7.41–7.66 (m, 10H), 7.08 (d, J = 7.6 Hz, 1H), 8.04 (s, 1H). ^{13}C NMR (101 MHz, $CDCl_3$) δ 19.5, 23.1, 27.2, 29.0, 51.9, 59.4, 66.8, 70.1, 84.6, 86.5, 88.5, 102.9, 128.2, 128.3, 130.4, 130.5, 132.0, 132.8, 135.4, 135.7, 140.0, 150.4, 163.1. HRMS (ESI) *m/z* Calcd for $C_{29}H_{37}N_5O_6SiNa$ $[M+Na]^+$ 602.2411, found 602.2396.

4.21. 4′-C-Azidopropyl-2′-O-methyluridine (14b)

1 M of TBAF solution in THF (7.74 mL, 7.74 mmol) was added to a solution of **13b** (2.99 g, 5.16 mmol) in THF (30 mL) under argon atmosphere and the mixture was stirred overnight at room temperature. The mixture was concentrated in vacuo. The residue was purified by chromatography on silica gel ($CHCl_3$/MeOH = 10:1) to give **14b** as a white solid (1.68 g, 4.94 mmol, 96%). ^{1}H NMR (600 MHz, DMSO-d_6) δ 1.55–1.67 (m, 4H), 3.27–3.29 (m, 2H), 3.32 (s, 3H), 3.42–3.45 (m, 2H), 3.98 (dd, J = 7.6 Hz and 4.8 Hz, 1H), 4.16 (t, J = 5.5 Hz, 1H), 5.13 (d, J = 6.2 Hz, 1H), 5.20 (d, J = 5.5 Hz, 1H), 5.67 (d, J = 8.3 Hz, 1H), 5.90 (d, J = 6.8 Hz, 1H), 7.89 (d, J = 8.2 Hz, 1H), 11.34 (s, 1H). ^{13}C NMR (101 MHz, DMSO-d_6) δ 22.8, 29.1, 51.3, 57.3, 64.2, 69.6, 82.5, 84.7, 88.0, 102.3, 140.7, 150.7, 163.0. HRMS (ESI) *m/z* Calcd for $C_{13}H_{19}N_5O_6K$ $[M+K]^+$ 380.0972, found 380.0976.

4.22. 5′-O-[Bis(4-methoxyphenyl)phenylmethyl]-4′-C-azidopropyl-2′-O-methyluridine (15b)

DMTrCl (2.51 g, 7.41 mmol) was added to a solution of **14b** (1.68 g, 4.94 mmol) in pyridine (17 mL) under argon atmosphere and the mixture was stirred for 5 h at room temperature. The mixture was extracted with H_2O and EtOAc. The organic layer was washed with saturated $NaHCO_3$ solution and brine, dried over Na_2SO_4 and concentrated in vacuo. The residue was purified by chromatography on silica gel (hexane/EtOAc = 2:1) to give **15b** as a white solid (3.12 g, 4.85 mmol, 98%). ^{1}H NMR (400 MHz, $CDCl_3$) δ 1.38–1.44 (m, 1H), 1.54–1.64 (m, 2H), 1.78–1.84 (m, 1H), 2.77 (d, J = 6.4 Hz, 1H), 3.17–3.22 (m, 2H), 3.34 (s, 2H), 3.57 (s, 3H), 3.80 (s, 6H), 3.92 (dd, J = 4.1 Hz and 5.96 Hz, 1H), 4.60 (t, J = 6.0 Hz, 1H), 5.22 (d, J = 8.2 Hz, 1H), 6.02 (d, J = 4.1 Hz, 1H), 6.84–7.36 (m, 13H), 7.82 (d, J = 8.2 Hz, 1H), 8.09 (s, 1H). ^{13}C NMR (101 MHz, $CDCl_3$) δ 14.3, 23.0, 29.3, 51.8, 55.4, 59.5, 60.5, 65.4, 70.6, 84.7, 86.8, 87.6, 88.0, 102.7, 113.5, 127.4, 128.2, 128.3, 130.3, 130.4, 134.9, 135.2, 140.3, 144.3, 150.3, 158.9, 159.0, 163.10. HRMS (ESI) *m/z* Calcd for $C_{34}H_{37}N_5O_8Na$ $[M+Na]^+$ 666.2540, found 666.2527.

4.23. 5′-O-[Bis(4-methoxyphenyl)phenylmethyl]-4′-C-trifluoroacetylaminopropyl-2′-O-methyluridine (17b)

PPh_3 (3.18 g, 12.1 mmol) and H_2O (3.50 mL) was added to a solution of **15b** (3.12 g, 4.85 mmol) in THF (62.4 mL) under argon atmosphere and the mixture was stirred for 20 h at 45 °C. The mixture was concentrated in vacuo to give crude **16b**. CF_3CO_2Et (1.74 mL, 14.5 mmol) and Et_3N (1.00 mL, 7.28 mmol) were added to a solution of **16b** in CH_2Cl_2 (30 mL) and the mixture was stirred 24 h at room temperature. The mixture was extracted with H_2O and EtOAc. The organic layer was washed with brine, dried over Na_2SO_4 and concentrated in vacuo. The residue was purified by chromatography on silica gel (hexane/EtOAc = 2:3) to give **17b** as a white solid (quant.). ^{1}H NMR (400 MHz, $CDCl_3$) δ 1.40–1.45 (m, 1H), 1.51–1.54 (m, 1H), 1.63–1.67 (m, 1H), 1.72–1.78 (m, 1H), 2.88 (d, J = 4.6 Hz, 1H), 3.25–3.28 (m, 2H), 3.30 (d, J = 10.5 Hz, 1H), 3.35 (d, J = 10.1 Hz, 1H), 3.54 (s, 3H), 3.80 (s, 6H), 4.03 (t, J = 5.0 Hz, 1H), 4.54 (t, J = 5.0 Hz, 1H), 5.26 (d, J = 8.2 Hz, 1H), 6.03 (d, J = 5.0 Hz, 1H), 6.66 (m, 1H), 6.84–7.55 (m, 13H), 7.74 (d, J = 8.2 Hz, 1H), 8.17 (s, 1H). ^{13}C NMR (101 MHz, $CDCl_3$) δ 14.3, 22.8, 29.4, 40.2, 55.4, 59.3, 60.5, 65.9, 70.7, 84.3, 86.4, 87.7, 87.9, 102.8, 113.5, 127.5, 128.2, 128.3, 130.2, 130.3, 132.1, 133.1, 134.8, 135.0, 140.2, 144.1, 150.4, 158.9, 159.0, 163.0. HRMS (ESI) *m/z* Calcd for $C_{36}H_{38}F_3N_3O_9K$ $[M+K]^+$ 752.2197, found 752.2207.

4.24. 5′-O-[Bis(4-methoxyphenyl)phenylmethyl]-4′-C-trifluoroaminopropyl-2′-O-methyl-3′-[2-cyanoethyl-N,N-bis(1-methylethyl) phosphoramidite]uridine (18b)

CEP-Cl (0.97 mL, 4.34 mmol) and DIPEA (1.90 mL, 10.9 mmol) were added to a solution of **17b** (1.55 g, 2.17 mmol) in THF (15 mL) under argon atmosphere and the mixture was stirred for 1.5 h at room temperature. The mixture was extracted with saturated $NaHCO_3$ solution and $CHCl_3$. The organic layer was washed with brine, dried over Na_2SO_4 and concentrated in vacuo. The residue was purified by chromatography on silica gel (hexane/EtOAc = 1:1) to give **18b** as a white solid (1.57 g, 1.71 mmol, 79%). ^{31}P NMR (243 MHz, $CDCl_3$) δ 150.57, 151.44. HRMS (ESI) *m/z* Calcd for $C_{45}H_{55}F_3N_5O_{10}PK$ $[M+K]^+$ 952.3276, found 952.3286.

4.25. Synthesis of the controlled pore glass support (21a) or (21b)

N,N-Dimethyl-4-aminopyridine (DMAP, 26.4 mg, 0.216 mmol) and succinic anhydride (43.2 mg, 0.432 mmol) were added to a solution of **17a** (74.5 mg, 0.108 mmol) in pyridine (1.0 mL) under argon atmosphere and the mixture was stirred for 27 h at room temperature. The mixture was extracted with H_2O and EtOAc. The organic layer was washed with sat. $NaHCO_3$ solution, brine, dried over Na_2SO_4 and concentrated in vacuo. The residue was purified by chromatography on silica gel ($CHCl_3$/MeOH = 15:1) to give **20a** as a white solid. Aminopropyl controlled pore glass (171 mg, CPG) and 1-ethyl-3-[3-(dimethylamino)propyl]carbodiimide hydrochloride (EDC, 21.9 mg, 0.114 mmol) were added to a solution of **20a**, and the mixture was kept at room temperature for 5 days. After the resin was washed with pyridine, 15 mL of capping solution (0.1 M DMAP in pyridine: Ac_2O 9:1) were added to the resin and the mixture was kept at room temperature for 2 days. The resin was washed with EtOH and acetone and was dried under vacuum to give solid support **21a**. The amount loaded nucleoside **20a** to the solid support is 44.1 μmol/g from calculation of released dimethoxytrityl cation by a solution of 70% $HClO_4$:EtOH (3:2, v/v). In a similar manner, the solid supports **21b** with **2.b** were obtained in 35.8 μmol/g of loading amounts.

4.26. Oligomer synthesis

The synthesis was carried out with DNA/RNA synthesizer by the phosphoramidite method. After the synthesis, the CPG beads were treated with 10% dimethylamine in MeCN for 5 min followed by rinse with MeCN to selectively remove cyanoethyl groups. Then, the oligomers were cleaved from CPG beads and deprotected by treated with concentrated NH_3 solution/40% methylamine (1:1, v/v) for 15 min at 65 °C. 2′-*O*-TBDMS groups were removed by $Et_3N{\cdot}3HF$ in DMSO at 65 °C for 1.5 h. The reaction quenched with 0.1 M TEAA buffer (pH 7.0) and the mixture desalted using Sep-Pak C18 cartridge. The oligonucleotides were purified by 20% PAGE containing 7 M urea to give highly purified ONs.

4.27. MALDI-TOF/MS analysis of ONs

The spectra were obtained with a time-of-flight mass spectrometer equipped with nitrogen laser (337 nm, 3 ns pulse). A solution of 3-hydroxypicolinic acid (3-HPA) and diammonium hydrogen citrate in H_2O was used as the matrix. Data of synthetic ONs: RNA **1** *m/z* = 4174.4 (calcd for $C_{138}H_{168}N_{28}O_{99}P_{12}$ $[M-H]^-$, 4175.63); RNA **2** *m/z* = 4304.30 (calcd for $C_{144}H_{183}N_{31}O_{99}P_{12}$ $[M-H]^-$, 4304.86); RNA **3** *m/z* = 4345.86 (calcd for $C_{147}H_{189}N_{31}O_{99}P_{12}$ $[M-H]^-$, 4346.93); RNA **4** *m/z* = 4388.00 (calcd for $C_{150}H_{195}N_{31}O_{99}P_{12}$ $[M-H]^-$, 4389.01); RNA **5** *m/z* = 3301.99 (calcd for $C_{99}H_{125}N_{25}O_{83}P_{10}$ $[M-H]^-$, 3302.91); RNA **6** *m/z* = 3345.31 (calcd for $C_{101}H_{130}N_{26}O_{83}P_{10}$ $[M-H]^-$, 3345.98); RNA **7** *m/z* = 3359.41 (calcd for $C_{102}H_{132}N_{26}O_{83}P_{10}$ $[M-H]^-$, 3360.01); RNA **8** *m/z* = 3373.47 (calcd for $C_{103}H_{134}N_{26}O_{83}P_{10}$ $[M-H]^-$, 3374.03); RNA **9** *m/z* = 3606.81 (calcd for $C_{110}H_{133}N_{55}O_{67}P_{10}$ $[M-H]^-$, 3607.30); RNA **10** *m/z* = 3582.40 (calcd for $C_{109}H_{132}N_{53}O_{68}P_{10}$ $[M-H]^-$, 3581.60); RNA **11** *m/z* = 3583.38 (calcd for $C_{109}H_{131}N_{52}O_{69}P_{10}$ $[M-H]^-$, 3582.58); RNA **12** *m/z* = 3622.50 (calcd for $C_{110}H_{132}N_{55}O_{68}P_{10}$ $[M-H]^-$, 3621.60); RNA **13** *m/z* = 6506.12 (calcd for $C_{194}H_{245}N_{65}O_{150}P_{20}$ $[M-H]^-$, 6505.84); RNA **14** *m/z* = 7353.56 (calcd for $C_{230}H_{272}N_{87}O_{153}P_{21}$ $[M-H]^-$, 7354.57); RNA **15** *m/z* = 6851.94 (calcd for $C_{210}H_{285}N_{73}O_{150}P_{20}$ $[M-H]^-$, 6851.44); RNA **16** *m/z* = 7569.94 (calcd for $C_{240}H_{297}N_{92}O_{153}P_{21}$ $[M-H]^-$, 7569.94); RNA **17** *m/z* = 6963.35 (calcd for $C_{218}H_{301}N_{73}O_{150}P_{20}$ $[M-H]^-$, 6962.62); RNA **18** *m/z* = 7638.62 (calcd for $C_{245}H_{307}N_{92}O_{153}P_{21}$ $[M-H]^-$, 7639.06); RNA **19** *m/z* = 7074.20 (calcd for $C_{226}H_{317}N_{73}O_{150}P_{20}$ $[M-H]^-$, 7075.83); RNA **20** *m/z* = 7709.50 (calcd for $C_{250}H_{317}N_{92}O_{153}P_{21}$ $[M-H]^-$, 7710.19); RNA **21** *m/z* = 6814.82 (calcd for $C_{203}H_{248}N_{86}O_{144}P_{20}$ $[M-H]^-$, 6816.11); RNA **22** *m/z* = 6520.22 (calcd for $C_{195}H_{247}N_{65}O_{150}P_{20}$ $[M-H]^-$, 6520.87); RNA **23** *m/z* = 6549.02 (calcd for $C_{196}H_{250}N_{66}O_{150}P_{20}$ $[M-H]^-$, 6549.92); RNA **24** *m/z* = 6560.70 (calcd for $C_{197}H_{252}N_{66}O_{150}P_{20}$ $[M-H]^-$, 6563.94); RNA **25** *m/z* = 6577.41 (calcd for $C_{198}H_{254}N_{66}O_{150}P_{20}$ $[M-H]^-$, 6577.97); RNA **26** *m/z* = 6521.16 (calcd for $C_{195}H_{247}N_{65}O_{150}P_{20}$ $[M-H]^-$, 6520.87); RNA **27** *m/z* = 6548.98 (calcd for $C_{196}H_{250}N_{66}O_{150}P_{20}$ $[M-H]^-$, 6549.92); RNA **28** *m/z* = 6562.83 (calcd for $C_{197}H_{252}N_{66}O_{150}P_{20}$ $[M-H]^-$, 6562.93); RNA **29** *m/z* = 6577.88 (calcd for $C_{198}H_{254}N_{66}O_{150}P_{20}$ $[M-H]^-$, 6577.97); RNA **30** *m/z* = 6520.52 (calcd for $C_{195}H_{247}N_{65}O_{150}P_{20}$ $[M-H]^-$, 6520.87); RNA **31** *m/z* = 6547.96 (calcd for $C_{196}H_{250}N_{66}O_{150}P_{20}$ $[M-H]^-$, 6549.92); RNA **32** *m/z* = 6560.41 (calcd for $C_{197}H_{252}N_{66}O_{150}P_{20}$ $[M-H]^-$, 6563.94); RNA **33** *m/z* = 6578.14 (calcd for $C_{198}H_{254}N_{66}O_{150}P_{20}$ $[M-H]^-$, 6577.97); RNA **34** *m/z* = 6519.83 (calcd for $C_{195}H_{247}N_{65}O_{150}P_{20}$ $[M-H]^-$, 6520.87); RNA **35** *m/z* = 6549.74 (calcd for $C_{196}H_{250}N_{66}O_{150}P_{20}$ $[M-H]^-$, 6549.92); RNA **36** *m/z* = 6562.89 (calcd for $C_{197}H_{252}N_{66}O_{150}P_{20}$ $[M-H]^-$, 6562.93); RNA **37** *m/z* = 6577.59 (calcd for $C_{198}H_{254}N_{66}O_{150}P_{20}$ $[M-H]^-$, 6577.97); RNA **38** *m/z* = 6520.51 (calcd for $C_{195}H_{247}N_{65}O_{150}P_{20}$ $[M-H]^-$, 6520.87); RNA **39** *m/z* = 6549.27 (calcd for $C_{196}H_{250}N_{66}O_{150}P_{20}$ $[M-H]^-$, 6549.92); RNA **40** *m/z* = 6560.44 (calcd for $C_{197}H_{252}N_{66}O_{150}P_{20}$ $[M-H]^-$, 6563.94); RNA **41** *m/z* = 6577.96 (calcd for $C_{198}H_{254}N_{66}O_{150}P_{20}$ $[M-H]^-$, 6577.97); RNA **42** *m/z* = 6520.23 (calcd for $C_{195}H_{247}N_{65}O_{150}P_{20}$ $[M-H]^-$, 6520.87); RNA **43** *m/z* = 6548.33 (calcd for $C_{196}H_{250}N_{66}O_{150}P_{20}$ $[M-H]^-$, 6549.92); RNA **44** *m/z* = 6562.89 (calcd for $C_{197}H_{252}N_{66}O_{150}P_{20}$ $[M-H]^-$, 6562.93); RNA **45** *m/z* = 6577.47 (calcd for $C_{198}H_{254}N_{66}O_{150}P_{20}$ $[M-H]^-$, 6577.97); RNA **46** *m/z* = 6635.92 (calcd for $C_{200}H_{260}N_{68}O_{150}P_{20}$ $[M-H]^-$, 6636.07); RNA **47** *m/z* = 6678.36 (calcd for $C_{203}H_{266}N_{68}O_{150}P_{20}$ $[M-H]^-$, 6678.14); RNA **48** *m/z* = 6720.48 (calcd for $C_{206}H_{272}N_{68}O_{150}P_{20}$ $[M-H]^-$, 6720.22); RNA **49** *m/z* = 6636.11 (calcd for $C_{200}H_{260}N_{68}O_{150}P_{20}$ $[M-H]^-$, 6636.07); RNA **50** *m/z* = 6678.36 (calcd for $C_{203}H_{266}N_{68}O_{150}P_{20}$ $[M-H]^-$, 6678.14); RNA **51** *m/z* = 6721.18 (calcd for $C_{206}H_{272}N_{68}O_{150}P_{20}$ $[M-H]^-$, 6720.22); RNA **52** *m/z* = 6635.31 (calcd for $C_{200}H_{260}N_{68}O_{150}P_{20}$ $[M-H]^-$, 6636.07); RNA **53** *m/z* = 6678.83 (calcd for $C_{203}H_{266}N_{68}O_{150}P_{20}$ $[M-H]^-$, 6678.14); RNA **54** *m/z* = 6719.67 (calcd for $C_{206}H_{272}N_{68}O_{150}P_{20}$ $[M-H]^-$, 6720.22); RNA **55** *m/z* = 6859.23 (calcd for $C_{205}H_{253}N_{87}O_{144}P_{20}$ $[M-H]^-$, 6859.18); RNA **56** *m/z* = 6873.75 (calcd for $C_{206}H_{255}N_{87}O_{144}P_{20}$ $[M-H]^-$, 6873.21); RNA **57** *m/z* = 6887.80 (calcd for $C_{207}H_{257}N_{87}O_{144}P_{20}$ $[M-H]^-$, 6887.23); RNA **58** *m/z* = 6859.09 (calcd for $C_{205}H_{253}N_{87}O_{144}P_{20}$ $[M-H]^-$, 6859.18); RNA **59** *m/z* = 6872.19 (calcd for $C_{206}H_{255}N_{87}O_{144}P_{20}$ $[M-H]^-$, 6873.21); RNA **60** *m/z* = 6887.74 (calcd for $C_{207}H_{257}N_{87}O_{144}P_{20}$ $[M-H]^-$, 6887.23); RNA **61** *m/z* = 6859.28 (calcd for $C_{205}H_{253}N_{87}O_{144}P_{20}$ $[M-H]^-$, 6859.18); RNA **62** *m/z* = 6872.97 (calcd for $C_{206}H_{255}N_{87}O_{144}P_{20}$ $[M-H]^-$, 6873.21); RNA **63** *m/z* = 6887.55 (calcd for $C_{207}H_{257}N_{87}O_{144}P_{20}$ $[M-H]^-$, 6887.23).

4.28. Thermal denaturation study

The solution containing 3.0 μM duplex in a buffer of 10 mM sodium phosphate (pH 7.0) containing 100 mM NaCl was heated at 100 °C, then cooled gradually to room temperature and used for the thermal denaturation study. Thermally induced transitions were monitored at 260 nm with a UV/Vis spectrometer fitted with temperature controller in quartz cuvettes with a path length of 1.0 cm. The sample temperature was increased by 0.5 °C/min. The thermodynamic parameters of the duplexes on duplex formation were determined by calculations based on the slope of a $1/T_m$ vs. ln ($C_T/4$) plot, where C_T (1, 3, 6, 12, 15, 21, 16, 30, and 60 μM) is the total concentration of single strands.

4.29. CD spectroscopy

All CD spectra were recorded at 25 °C. The following instrument settings were used: resolution, 0.1 nm; response, 1.0 s; speed, 50 nm/min; accumulation, 10.

4.30. NMR measurements

The ON7 was dissolved in 10 mM sodium phosphate (pH 7.0) containing 100 mM NaCl. The final concentration of the RNA was 0.5 mM. NMR spectra were measured using Bruker AVANCE 600 spectrometer. Spectra were recorded at probe temperature of 45 °C. Non-exchangeable proton resonances were assigned by TOCSY (mixing time of 50 ms) and NOESY (mixing times of 100 and 400 ms) in D_2O.

4.31. Molecular modeling study

The initial structure of uridine and three 4′-*C*-amino-alkyl-2′-*O*-methyl-uridine nucleosides **1**, **2** and **3** were modeled using the BIOPOYMER module implemented in SYBYL package. The geometry of each nucleoside was optimized using Gaussian09[40] at the HF/6-31G* level of theory and RESP charges[41] were derived using the Antechamber RESP fitting procedure. The general AMBER force field (GAFF)[42] adopted to obtain the force field parameters of each nucleosides. Each nucleotide was solvated in TIP3P water model[43] using the LEaP module of AMBER 14[44] and placed with periodic boundary conditions in a cubic box with side length 42.0 Å. Counter-ion (Cl−) was added into the solution to neutralize the charge of the systems. The solvent was energy minimized by 2500 steps of the steepest descent method and then followed by 2500 steps of the conjugate gradient method, applying a restraint force constant of 2 kcal/(mol Å^2) to the nucleoside. After that, the entire system was relaxed with 5000 steps of energy minimization without any restrains. Initially, the temperature of system was increased gradually from 0 to 300 K over a period of 100 ps of NVT dynamics. This was followed by 50 ps of NPT equilibration at 300 K and 1 atm pressure. After the equilibration phase, 100 ns productive MD simulations were performed in an NPT ensemble at 1 atom and 300 K without any restrains. During all MD simulations, a time step of 2 fs was used. The cut-off of the van der Waals interaction was set to be 10 Å, the SHAKE algorithm[45] was used to constrain all bonds involving hydrogen atoms and particle-mesh Ewald (PME)[46] was used long-range electrostatic interactions. The temperature is regulated by the Langevin dynamics[47] with a collision frequency of 1.0 ps^{-1}. All of the MD simulations were performed using the SANDER module of AMBER 14 package. Trajectory analysis was done using the cpptraj module in AMBER 14 and examined visually using VMD 1.9.2.

4.32. Dual luciferase assay

HeLa cells were transfected with the psiCHECK-2 (Promega) reporter and the pcDNA3.1 containing a hygromycin resistance gene (Thermo Fisher Scientific). Cells were cultured in the presence of 0.5 mg/mL hygromycin for one week. Stable HeLa-psiCHECK-2 cells expressing both *Renilla* and firefly luciferases were grown in Dulbecco's Modified Eagle Medium (d-MEM) supplemented with 10% bovine serum (BS) and 0.25 mg/mL hygromycin at 37 °C. HeLa-psiCHECK-2 cells (8.0×10^4/mL) were cultured on a 96-well plate (100 μL/well) for 24 h and transfected with siRNA targeting the *Renilla* luciferase gene using lipofectamine RNAi max in Opti-MEM I reduced serum medium. Transfection without siRNA was used as a control. After 1 h, d-MEM (50 μL) containing 10% BS was added to each well and cells was further incubated for another 24 h. The activities of *Renilla* and firefly luciferases in the cells were determined with Dual-Luciferase Reporter Assay System (Promega) according to a manufacture's protocol. The activity of *Renilla* luciferase was normalized by the firefly luciferase activity. The results were confirmed by at least three independent transfection experiments with two cultures each and are expressed as the average from four experiments as mean ± SD.

4.33. Stability in serum

Fluorescein labeled ONs and siRNA (600 pmol) were dissolved in 10 μL buffer of 10 mM sodium phosphate (pH 7.0) containing 100 mM NaCl and the solutions were heated at 100 °C, then cooled gradually to room temperature and used for the serum stability test. 90 μL bovine serum was added and the mixture was incubated at 37 °C for the required time. Aliquots of 10 μL were diluted with a stop solution (65 mM EDTA 12% glycerol 8.0 μL). Samples were subjected to electrophoresis in 15% polyacrylamide-TBE under non-denaturing conditions and quantified by Luminescent Image analyzer LAS-4000 (Fujifilm).

Acknowledgement

This work was supported by the Japan Agency for Medical Research and Development (AMED) through its Funding Program for Basic Science and Platform Technology Program for Innovative Biological Medicine, development of siRNA conjugates with tissue-specific delivery functions. The authors thank Professor Yoko Hirata (Gifu University) for supplying cells and giving technical advice.

A. Supplementary data

Supplementary data (UV melting profiles and graphical data of $1/T_m$ vs. ln ($C_T/4$) plots. Additional data from molecular modeling studies. 2D NOESY spectrum of 5′-CGCGAAU**2**CGCG-3′. Sequences of siRNAs and their abilities to suppress gene expression. ^{1}H and ^{13}C NMR spectra of compounds **5–19** and ^{31}P NMR spectra of compounds **18a** and **18b**) associated with this article can be found, in the online version, at http://dx.doi.org/10.1016/j.bmc.2018.05.025.

References

1. Fire A. Xu; S., Montgomery, M.K.; Kostas, S. A.; Driver, S. E.; Mello, C. C. *Nature.* 1998;391:806–811.
2. Ryther RC, Flynt AS, Phillips JA, Patton JG. *Gene Ther.* 2005;12:5–11.
3. Lam JK, Chow MY, Zhang Y, Leung SW. *Mol Ther Nucleic Acids.* 2015;4:e252.
4. Kawamata T, Tomari Y. *Trends Biochem Sci.* 2010;35:368–376.
5. Filipowicz W. *Cell.* 2005;122:17–20.
6. Schwarz DS, Hutvagner G, Du T, Xu Z, Aronin N, Zamore PD. *Cell.* 2003;115:199–208.
7. Khvorova A, Reynolds A, Jayasena SD. *Cell.* 2003;115:209–216.
8. Garba AO, Mousa SA. *Ophthalmol. Eye Dis..* 2010;2:75–83.
9. Golkar N, Samani SM, Tamaddon AM. *Int J Pharm.* 2016;510:30–41.
10. Wisniewska-Kruk J, van der Wijk AE, van Veen HA, et al. *Am J Pathol.* 2016;186:1044–1054.
11. Burnett JC, Rossi JJ, Tiemann K. *Biotechnol J.* 2011;6:1130–1146.
12. Turner JJ, Jones SW, Moschos SA, Lindsay MA, Gait MJ. *Mol BioSyst.* 2007;3:43–50.
13. Aagaard L, Rossi JJ. *Adv Drug Deliv Rev.* 2007;59:75–86.
14. Ku SH, Jo SD, Lee YK, Kim K, Kim SH. *Adv Drug Deliv Rev.* 2016;104:16–28.
15. Sioud M. *Eur J Immunol.* 2006;36:1222–1230.
16. Lamond AI, Sproat BS. *FEBS Lett.* 1993;325:123–127.
17. Choung S, Kim YJ, Kim S, Park HO, Choi YC. *Biochem Biophys Res Commun.* 2006;342:919–927.
18. Allerson CR, Sioufi N, Jarres R, et al. *J Med Chem.* 2005;48:901–904.

19. Milton S, Honcharenko D, Rocha CSJ, Moreno PMD, Smith CIE, Strömberg R. *Chem Commun.* 2015;51:4044–4047.
20. Teplova M, Wallace ST, Tereshko V, et al. *PNAS.* 1999;96:14240–14245.
21. Noe CR, Winkler J, Urban E, Gilbert M, Haberhauer G, Brunar H. *Nucleosides Nucleotides Nucleic Acids.* 2005;24:1167–1185.
22. Wang Y, Juranek S, Li H, et al. *Nature.* 2009;461:754–761.
23. Frank F, Sonenberg N, Nagar B. *Nature.* 2010;465:818–822.
24. Ueno Y, Nagasawa Y, Sugimoto I, et al. *J Org Chem.* 1998;63:1660–1667.
25. Kanazaki M, Ueno Y, Shuto S, Matsuda A. *J Am Chem Soc.* 2000;122:2422–2432.
26. Matsuda A, Ueno Y, Takenaka A. *Frontiers in Nucleosides and Nucleic Acids.* HL Press; 2004:549–576.
27. Gore KR, Nawale GN, Harikrishna S, et al. *J Org Chem.* 2012;77:3233–3245.
28. Morita K, Takagi M, Hasegawa C, et al. *Bioorg Med Chem.* 2003;11:2211–2226.
29. Varghese OP, Barman J, Pathmasiri W, Plashkevych O, Honcharenko D, Chattopadhyaya J. *J Am Chem Soc.* 2006;128:15173–15187.
30. Honcharenko D, Varghese OP, Plashkevych O, Barman J, Chattopadhyaya J. *J Org Chem.* 2006;71:299–314.
31. Jin S, Miduturu CV, McKinney DC, Silverman SK. *J Org Chem.* 2005;70:4284–4299.
32. Hobartner C, Kreutz C, Flecker E, et al. *Monatsh Chem.* 2003;134:851–873.
33. Varani G, Aboul-ela F, Allain FHT. *Progr. NMR Spectr.* 1996;29 51–27.
34. Chou SH, Flynn P, Reid B. *Biochemistry.* 1989;28:2422–2435.
35. Masliah G, Maris C, König SLB, et al. *EMBO J.* 2018:e97089.
36. Altona C, Sundaralingam M. *J Am Chem Soc.* 1972;94:8205–8212.
37. Wang Y, Juranek S, Li H, et al. *Nature.* 2009;461:54–61.
38. Elkayam E, Kuhn CD, Tocilj A, et al. *Cell.* 2012;150:100–110.
39. Harikrishna S, Pradeepkumar PI. *J Chem Inf Model.* 2017;57:883–896.
40. Frisch MJ, Trucks GW, Schlegel HB, Scuseria GE, Robb MA, Cheeseman JR, Scalmani G, Barone V, Petersson GA, Nakatsuji H, Li X, Caricato M, Marenich A, Bloino J, Janesko BG, Gomperts R, Mennucci B, Hratchian HP, Ortiz JV, Izmaylov AF, Sonnenberg JL, Williams-Young D, Ding F, Lipparini F, Egidi F, Goings J, Peng B, Petrone A, Henderson T, Ranasinghe D, Zakrzewski VG, Gao J, Rega N, Zheng G, Liang W, Hada M, Ehara M, Toyota K, Fukuda R, Hasegawa J, Ishida M, Nakajima T, Honda Y, Kitao O, Nakai H, Vreven T, Throssell K, Montgomery Jr JA, Peralta JE, Ogliaro F, Bearpark M, Heyd JJ, Brothers E, Kudin KN, Staroverov VN, Keith T, Kobayashi R, Normand J, Raghavachari K, Rendell A, Burant JC, Iyengar SS, Tomasi J, Cossi M, Millam JM, Klene M, Adamo C, Cammi R, Ochterski JW, Martin RL, Morokuma K, Farkas O, Foresman JB, Fox DJ. *Gaussian 09, Revision A.02.* Wallingford CT: Gaussian Inc.; 2016.
41. Cornell WD, Cieplak P, Bayly CI, Kollman PA. *J Am Chem Soc.* 1993;115:9620–9631.
42. Wang J, Wolf RM, Caldwell JW, Kollman PA, Case DA. *J Comput Chem.* 2004;25:1157–1174.
43. Jorgensen WL, Chandrasekhar J, Madura JD, Impey RW, Klein ML. *J Chem Phys.* 1983;79:926–935.
44. Case DA, et al. *AMBER 14.* San Francisco: University of California; 2014.
45. Ryckaert JP, Ciccotti G, Berendsen HJC. *J Comput Phys.* 1977;23:327–341.
46. Darden T, York DM, Pedersen LG. *J Chem Phys.* 1993;98:10089–10092.
47. Pastor RW, Brooks BR, Szabo A. *Mol Phys.* 1988;65:1409–1419.